Thermodynamic and Transport Properties of Strongly-Coupled Degenerate Electron-Ion Plasma by First-Principle Approaches

Levashov P.R.

Joint Institute for High Temperatures, Moscow, Russia
Moscow Institute of Physics and Technology, Dolgoprudny, Russia

*pasha@ihed.ras.ru

In collaboration with: Minakov D.V.
Knyazev D.V.
Chentsov A.V.
Khishchenko K.V.

JIHT RAS

Outline

- Strongly coupled degenerate plasma
- Ab-initio calculations
- Quantum-statistical models
- Density functional theory
- Quantum molecular dynamics
- Path-Integral Monte Carlo
- Wigner dynamics
- Conclusions

JIHT RAS

Ab-initio calculations

- Thermodynamic, transport and optical properties
- Use the following information:
  - fundamental physical constants
  - charge and mass of nuclei
  - thermodynamic state

JIHT RAS

Extreme States of Matter

- Kirzhnits D.A., Phys. Usp., 1971
- Atomic system of units:
  - $m_e = \hbar = a_0 = 1$
- Extreme States of Matter (Kalitkin N.N.)
  - $P = e^2/a_0^4 = 294.2\ \text{Mbar}$
  - $E = e^2/a_0 = 27.2\ \text{eV}$
  - $V = a_0^3 = 0.1482\ \text{A}$
- Hypervelocity impact, laser, electronic, ionic beams, powerful electric current pulse etc.

JIHT RAS

Coupling and Degeneracy in Plasma

- Coupling parameter:

$$\Gamma = \frac{U_{pot}}{E_{kin}} = \frac{e^2}{k_B T \langle r \rangle}$$ (for electronic subsystem)

$\Gamma \gg 1$ - Strong coupling

- Degeneracy parameter

$$n_e \lambda_e^3, \lambda_e^2 = \frac{2\pi\hbar^2}{m_e k_B T}$$

$n_e \lambda_e^3 \gg 1$ - Strong degeneracy

$\Gamma \gg 1$
$n_e \lambda_e^3 \gg 1$ - Strongly coupled degenerate non-relativistic plasma (warm dense matter)

EOS: Traditional Form

Adiabatic (Born-Oppenheimer) approximation ($m_e << m_i$)

$$F(V,T) = F_e\left(V,T,\left\{R_t^0\right\}\right) + F_n\left(V,T,\left\{R_t^0\right\}\right)$$

Free energy of electrons in the field of fixed ions

Free energy of ions interacting with potential depending on V and T

Traditional form of semiempirical EOS. Free energy

$$F(V,T) = F_c(V) + F_i(V,T) + F_e(V,T)$$

Cold curve

Thermal contribution of atoms and ions

Thermal contribution of electrons

Semiempirical expressions

DFT, mean atom models

Mean atom models or DFT calculations might help to decrease the number of fitting parameters

Electronic Contribution to Thermodynamic Functions: Hierarchy of Models

- Exact solution of the 3D multi-particle Schrödinger equation
- Atom in a spherical cell
- Hartree-Fock method (1-electron wave functions)
- Hartree-Fock-Slater method
- Hartree method (no exchange)
- Thomas-Fermi method
- Ideal Fermi-gas

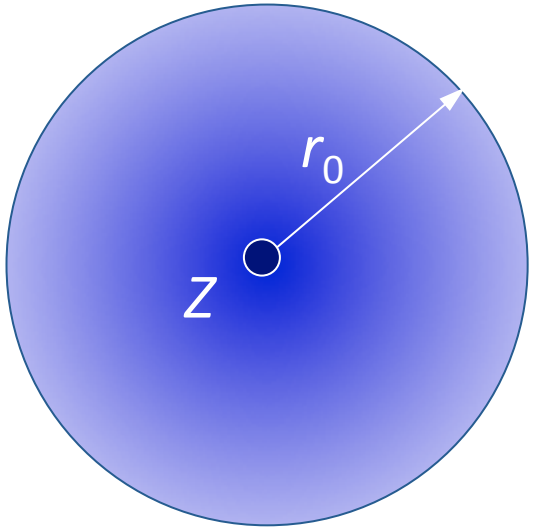

$$\frac{4}{3}\pi r_0^3 = \frac{1}{n}$$

Finite-Temperature Thomas-Fermi Model

- The simplest mean atom model
- The simplest (and fully-determined) DFT model
- Correct asymptotic behavior at low *T* and *V* (ideal Fermi-gas) and at high *T* and *V* (ideal Boltzmann gas)

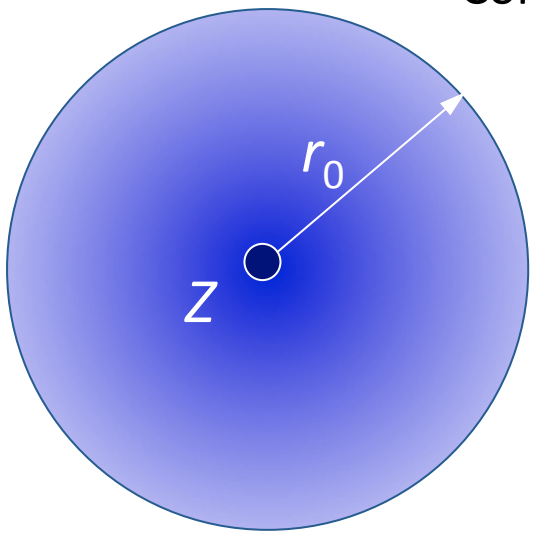

Poisson equation

$$\Delta V = -4\pi Z\delta(r) + \frac{2}{\pi}(2\theta)^{3/2} I_{1/2}\left(\frac{V(r)+\mu}{\theta}\right)$$

$$(0 \le r < r_0)$$

$$rV(r)\big|_{r=0} = Z \qquad V(r_0) = 0 \qquad \frac{dV(r)}{dr}\bigg|_{r=r_0} = 0$$

Thomas-Fermi model is realistic but crude at relatively low temperatures and pressures. Thermal contributions to thermodynamic functions is a good approximation.

Feynman R., Metropolis N., Teller E. // Phys. Rev. 1949. V.75. P.1561.

HARTREE-FOCK-SLATER MODEL AT $T>0$

Nikiforov A.F., Novikov V.G., Uvarov V.B. Quantum-statistical models of high-temperature plasma. M.: Fizmatlit, 2000.

Atom with mean populations

$$N_{nl} = \frac{2(2l+1)}{1+\exp(\varepsilon_{nl} - \mu/\theta)}$$

ε_{nl} – energy levels in $V(r)$

From the radial Schrödinger equation

Potential:

$$V(r) = V_c(r) + V_{ex}(r)$$

Poisson equation solution:

$$V_c(r) = \frac{Z}{r} - 4\pi\left[\frac{1}{r}\int_0^r r'^2\,\rho(r')dr' + \int_r^{r_0} r'\rho(r')dr'\right]$$

Exchange potential:

$$V_{ex}(r) = \frac{\pi r(r)}{\theta}\left[1 + 5.7\frac{\rho(r)}{\theta^{3/2}} + \frac{\pi^4}{3}\frac{\rho^2(r)}{\theta^3}\right]^{-1/3}$$

Iterative procedure for determination of $\rho(r)$, ε_{nl} and $V(r)$

RADIAL ELECTRON DENSITY $r^2\rho(r)$ BY HARTREE-FOCK-SLATER MODEL

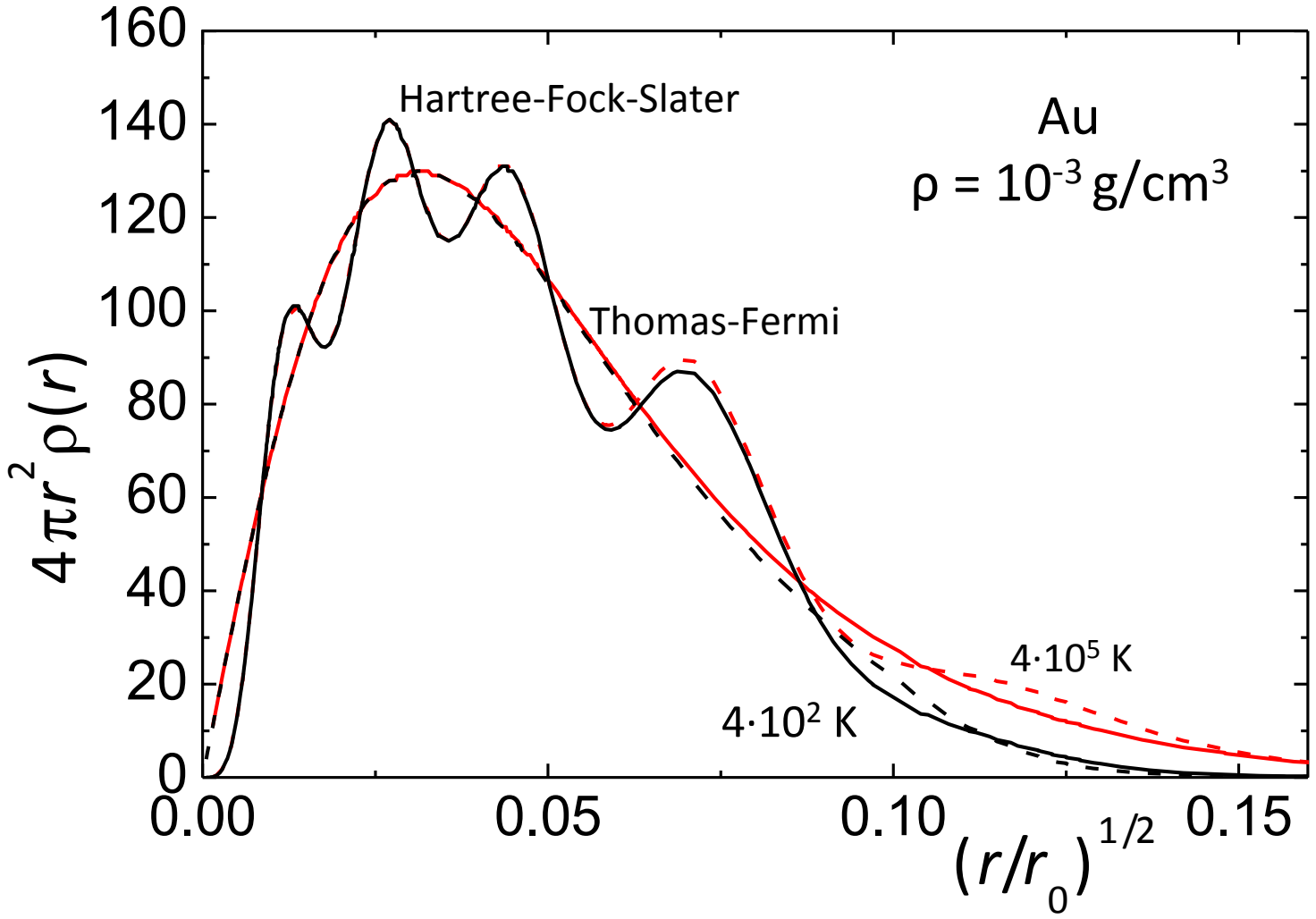

JIHT RAS

Density Functional Theory

- Thomas-Fermi theory is the density functional theory:

kinetic energy

external potential

$$E_{TF}[n] = C_1 \int d^3 r n(\mathbf{r})^{5/3} + \int d^3 r V_{ext}(\mathbf{r}) n(\mathbf{r}) +$$

$$C_2 \int d^3 r n(\mathbf{r})^{4/3} + \frac{1}{2} d^3 r d^3 r' \frac{n(\mathbf{r}) n(\mathbf{r}')}{|\mathbf{r} - \mathbf{r}'|}$$

exchange energy

Hartree energy

- Is it a general property?

JIHT RAS

Density Functional Theory

For systems with Hamiltonian

$$\hat{H} = -\frac{1}{2}\sum_i \nabla_i^2 + \sum_i V_{\text{ext}}(\mathbf{r}_i) + \frac{1}{2}\sum_{i\neq j}\frac{e^2}{|\mathbf{r}_i - \mathbf{r}_j|}$$

the following theorems are valid:

Theorem 1. For any system of interacting particles in an external potential $V_{\text{ext}}(\mathbf{r})$ the potential $V_{\text{ext}}(\mathbf{r})$ is determined uniquely, except for a constant, by the ground state particle density of electrons $n_0(\mathbf{r})$.
Therefore, all properties are completely determined given only the ground state electronic density $n_0(\mathbf{r})$.

Theorem 2. A universal functional for the energy $E[n]$ in terms of the density $n(\mathbf{r})$ can be defined, valid for any external potential $V_{\text{ext}}(\mathbf{r})$. For any particular $V_{\text{ext}}(\mathbf{r})$, the exact ground state energy of the system is the global minimum value of this functional, and the density $n(\mathbf{r})$ that minimizes the functional is the exact ground state density $n_0(\mathbf{r})$.

Hohenberg, Kohn, 1964

Kohn-Sham Functional

The system of interacting particles is replaced by the system of non-interacting particles:

$$E_{KS}[n] = T_s[n] + \int d\mathbf{r} V_{ext}(\mathbf{r}) n(\mathbf{r}) + E_{Hartree}[n] + E_{II} + E_{XC}[n]$$

kinetic energy

ion-ion interaction

exchange-correlation functional

All many-body effects of exchange and correlation are included into $E_{XC}[n]$

$$E_{XC}[n] = \left\langle \hat{T} \right\rangle - T_s[n] + \left\langle \hat{V}_{\text{int}} \right\rangle - E_{Hartree}[n]$$

true system

non-interacting system

The minimization of E_{KS} leads to the system of Kohn-Sham equations

Kohn, Sham, 1965

JIHT RAS

Minimization in HFS and DFT

- In Hartree-Fock(-Slater) method we find

$$\min_{\Psi_i(\mathbf{r})} \Omega\left[\Psi_i(\mathbf{r})\right]$$

- In DFT we find

$$\min_{n(\mathbf{r})} \Omega\left[n(\mathbf{r})\right]$$

Density Functional Theory: All-Electron and Pseudopotential Approaches

Full-potential approach: all electrons are taken into account (FP-LMTO)

(S. Yu. Savrasov, PRB **54** 16470 (1996),
G. V. Sin'ko, N. A. Smirnov, PRB **74** 134113 (2006)

At $T > 0$: occupancies are $f(\varepsilon, \rho, T) = 1 / \left\{1 + \exp\left[(\varepsilon - \mu(\rho, T)) / T\right]\right\}$

Pseudopotential approach: the core is replaced by a pseudopotential, the Kohn-Sham equations are solved only for valent electrons (VASP)

G. Kresse and J. Hafner, Phys. Rev. B **47**, 558 (1993); **49**, 14251 (1994).
G. Kresse and J. Furthmuller, Phys. Rev. B **54**, 11169 (1996).

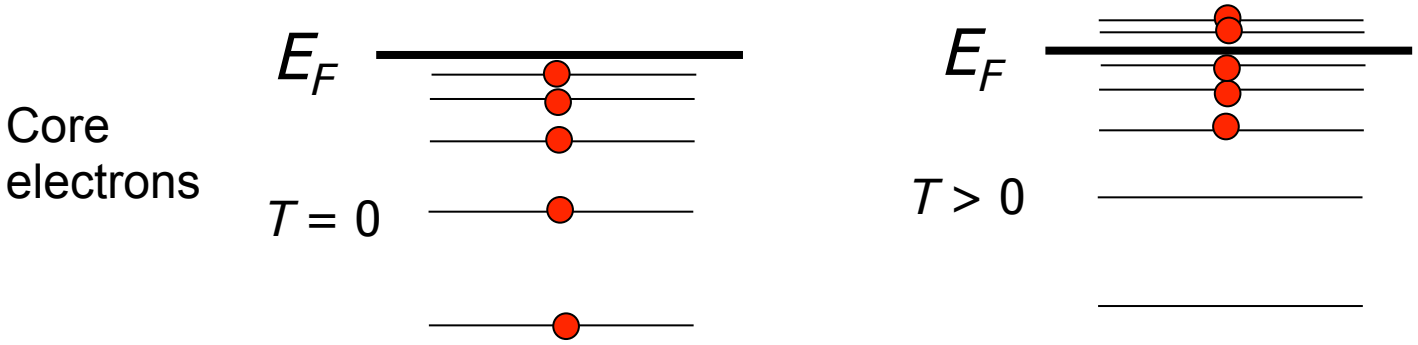

Calculations were made in the unit cell at fixed ions and heated electrons

Aluminum. Cold Curve

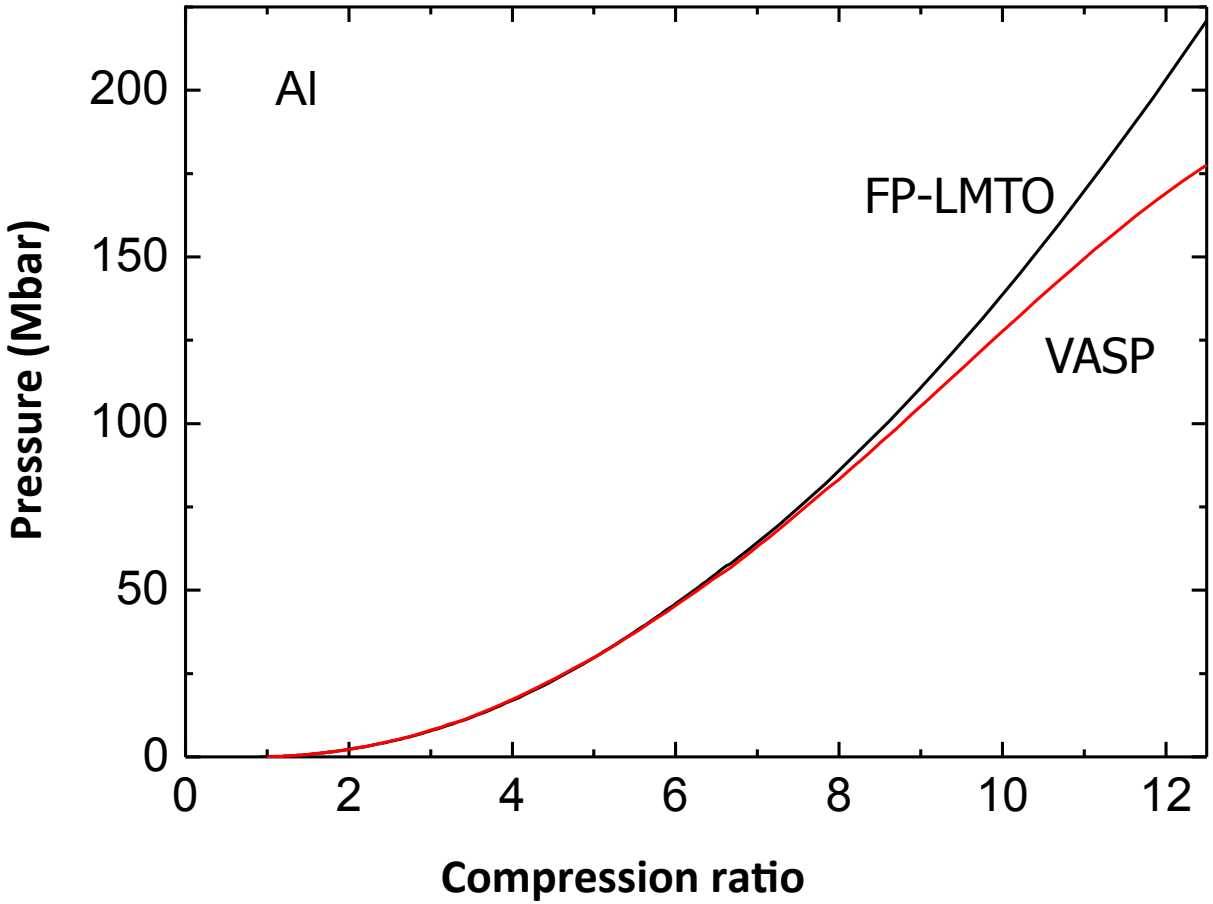

Al is more compressible in VASP calculations than in FP-LMTO

Levashov P.R. et al., JPCM **22** (2010) 505501

Potassium. Cold Curve

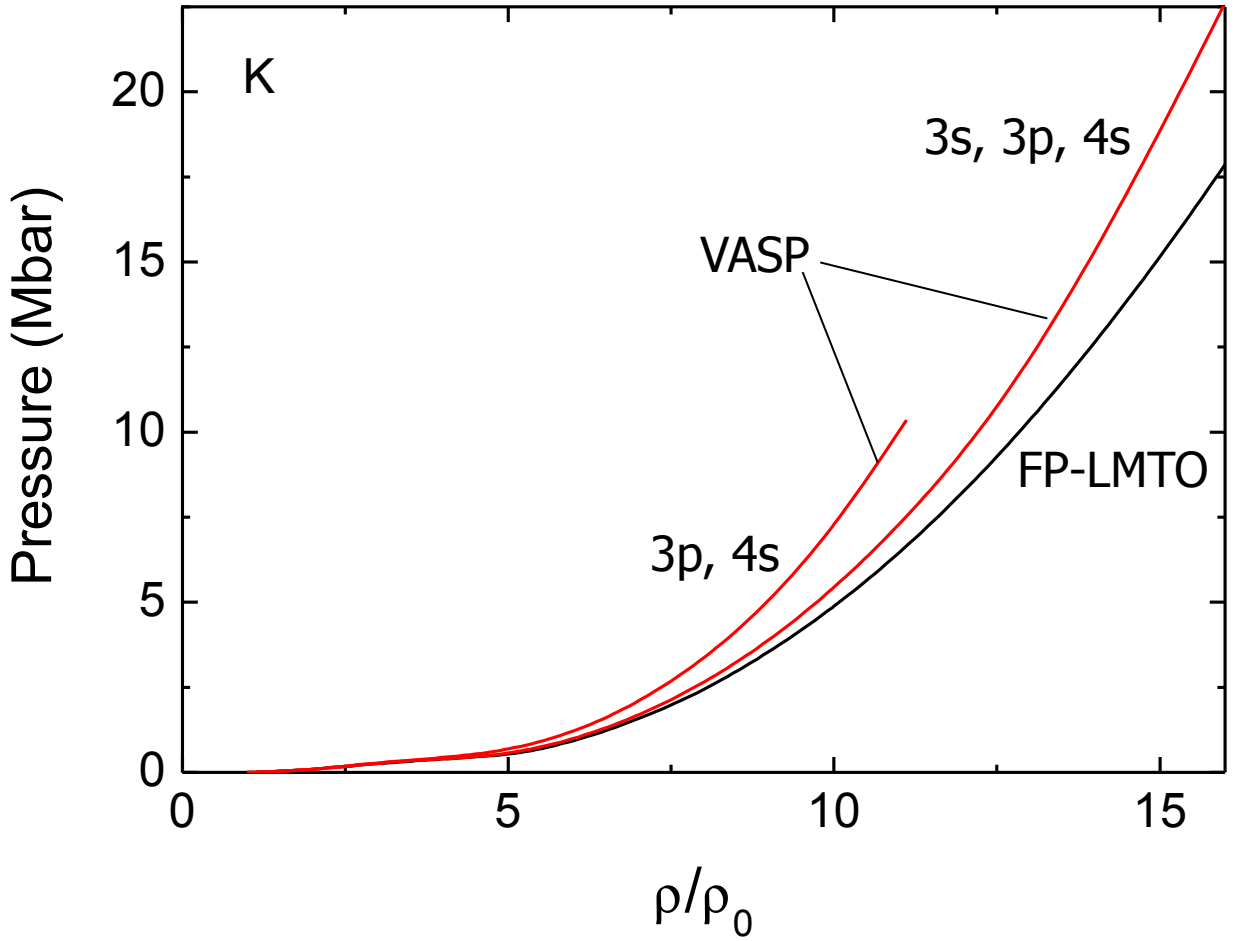

K is less compressible in VASP calculations than in FP-LMTO

Less number of valent electrons leads to bigger disagreement with FP-LMTO

Levashov P.R. et al., JPCM **22** (2010) 505501

DFT-calculations of $F_e(T_e, V)$

Why can we use DFT for thermodynamic properties of electrons?

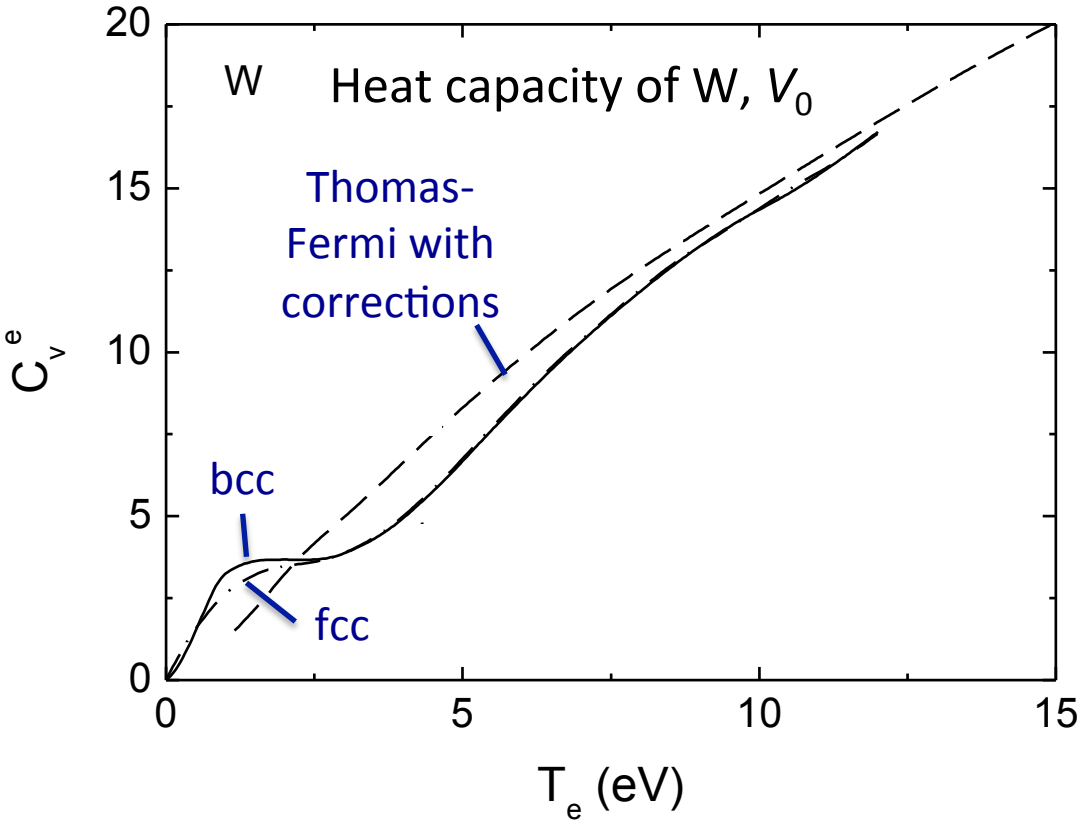

$$P_T^e = -\rho^2 \left. \frac{\partial F_T^e(\rho, T_e)}{\partial \rho} \right|_{T_e} - P_c$$

$$C_V^e = \left[\frac{\partial E_T^e(\rho, T_e)}{\partial T_e} \right]_V$$

24x24x24 mesh of k-points

N_{bands} = 94

E_{cut} = 1020 eV

- Cold ions, hot electrons
- Heat capacity is very close for fcc and bcc structures of W
- It should be close to unordered phase at the same density

Tungsten, $T_i = 0$, $V = V_0$. Electron Heat Capacity

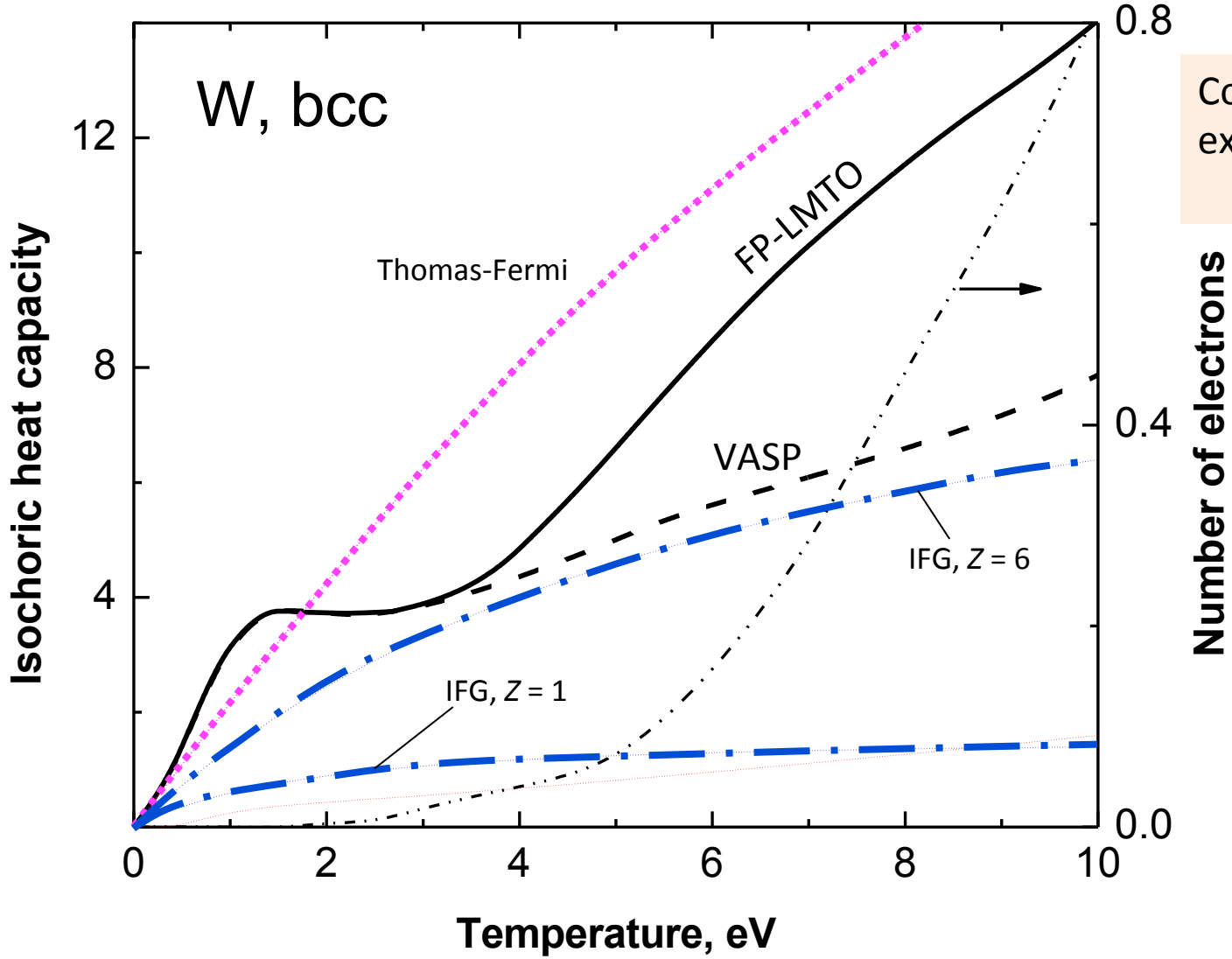

Core electrons become excited at ~3 eV

Levashov P.R. et al., JPCM **22** (2010) 505501

Tungsten, $T_i = 0$, $V = V_0$. Thermal Pressure

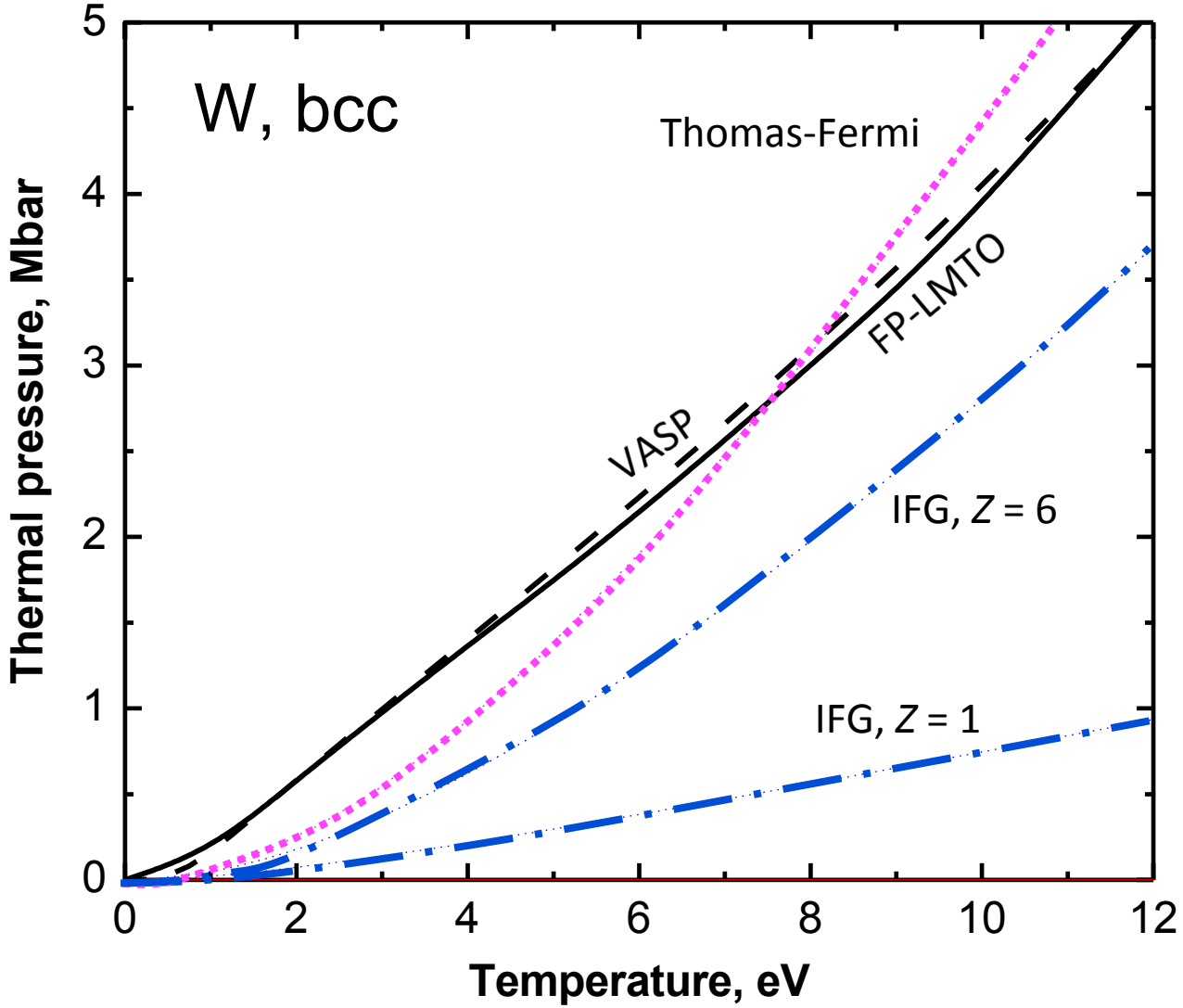

- Pressure is determined by free electrons only
- Interaction of electrons should be taken into account

Levashov P.R. et al., JPCM **22** (2010) 505501

Thermal contribution of ions

Ab-initio molecular dynamics (AIMD) simulations

$$F(V,T) = F_c(V) + F_i(V,T) + F_e(V,T)$$

$$F_{AIMD}(V,T) - F_e(V,T) - F_c(V) + F_{ions,kin}(V,T)$$

From AIMD — From AIMD — From DFT — Analytic expression

But it's better to use AIMD to calibrate the EOS by changing fitting parameters

Desjarlais M., Mattson T.R., Bonev S.A., Galli G., Militzer B., Holst B., Redmer R., Renaudin P., Clerouin J. and many others use AIMD to compute EOS for many substances

JIHT RAS

Details of the AIMD simulations

- We use **VASP** (Vienna Ab Initio Simulation Package) - package for performing ab-initio quantum-mechanical molecular dynamics (MD) using pseudopotentials and a plane wave basis set.
- Generalized Gradient Approximation (**GGA**) for Exchange and Correlation functional
- Ultrasoft Vanderbilt pseudopotentials (**US-PP**)
- One point (**Γ-point**) in the Brillouin zone
- The QMD simulations were performed for **108 atoms** of Al
- The dynamics of Al atoms was simulated within **1 ps** with **2 fs time step**
- The electron temperature was equal to the temperature of ions through the **Fermi–Dirac** distribution
- $0.1 < \rho / \rho_0 < 3$, $T < 75000$ K

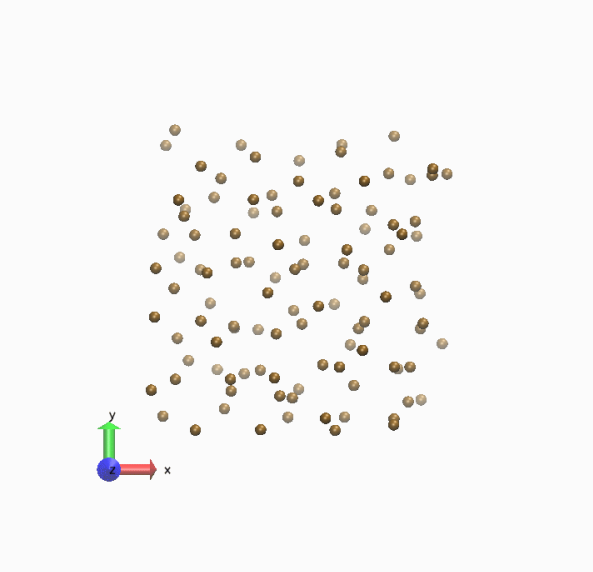

G. Kresse and J. Hafner, Phys. Rev. B **47**, 558 (1993); **49**, 14251 (1994).
G. Kresse and J. Furthmuller, Phys. Rev. B **54**, 11169 (1996).

Al, ionic configurations

Full energy during the simulations

Normal conditions, solid phase

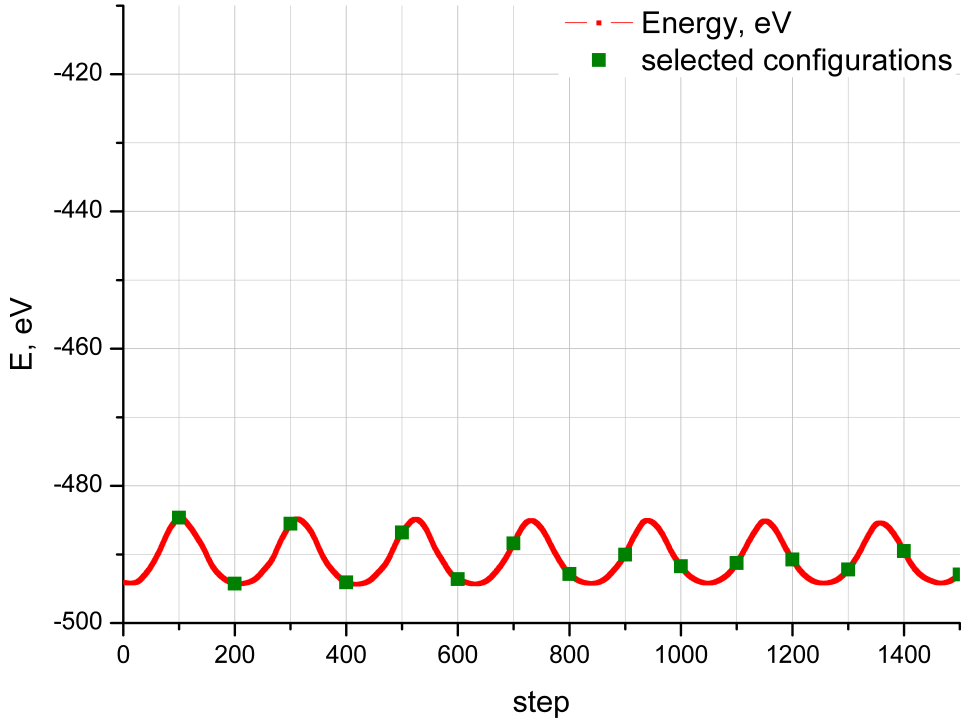

T=1550 K; ρ=2.23 g/cm^3; liquid phase

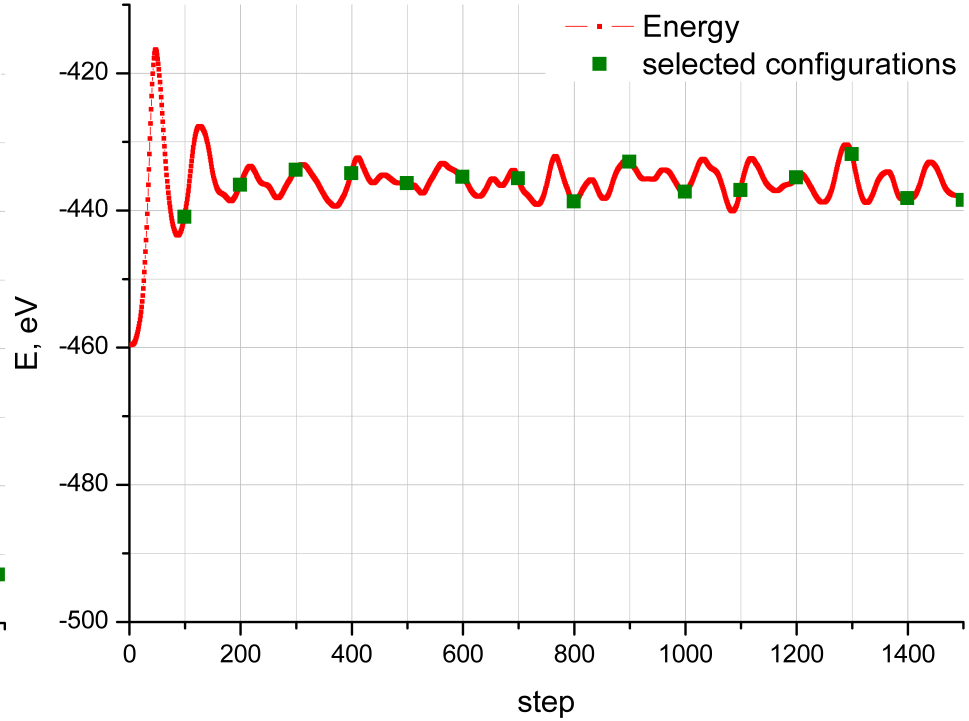

108 atoms US pseudopotential; 1 k-point in the Brillouin zone; cut-off energy 100 eV; 1 step – 2 fs

Configurations for electrical conductivity calculations are taken after equilibration

Isotherm *T* = 293 K for Al

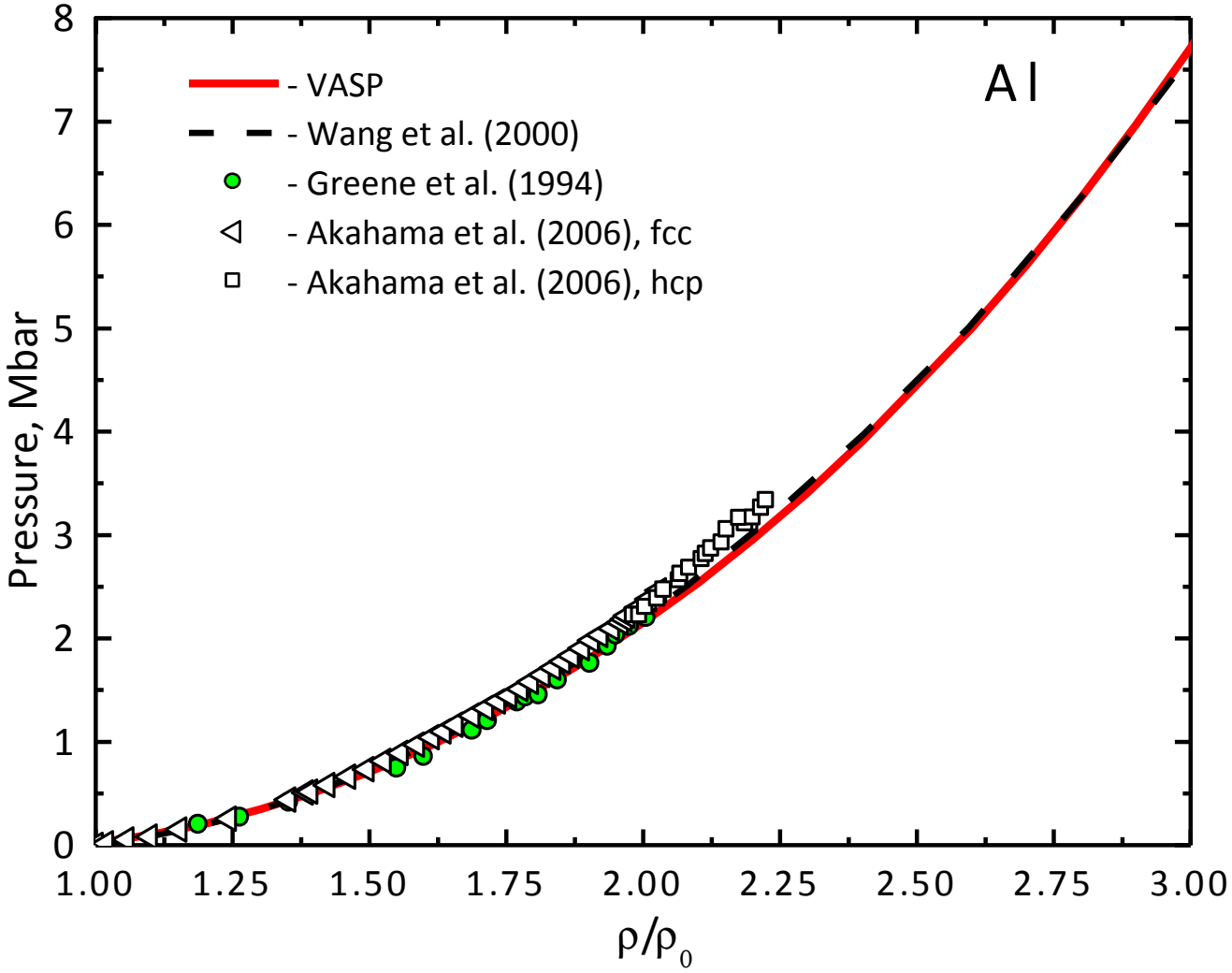

QMD results show good agreement with experiments and calculations for fcc.

Shock Hugoniots of Al

Pressure – compression ratio

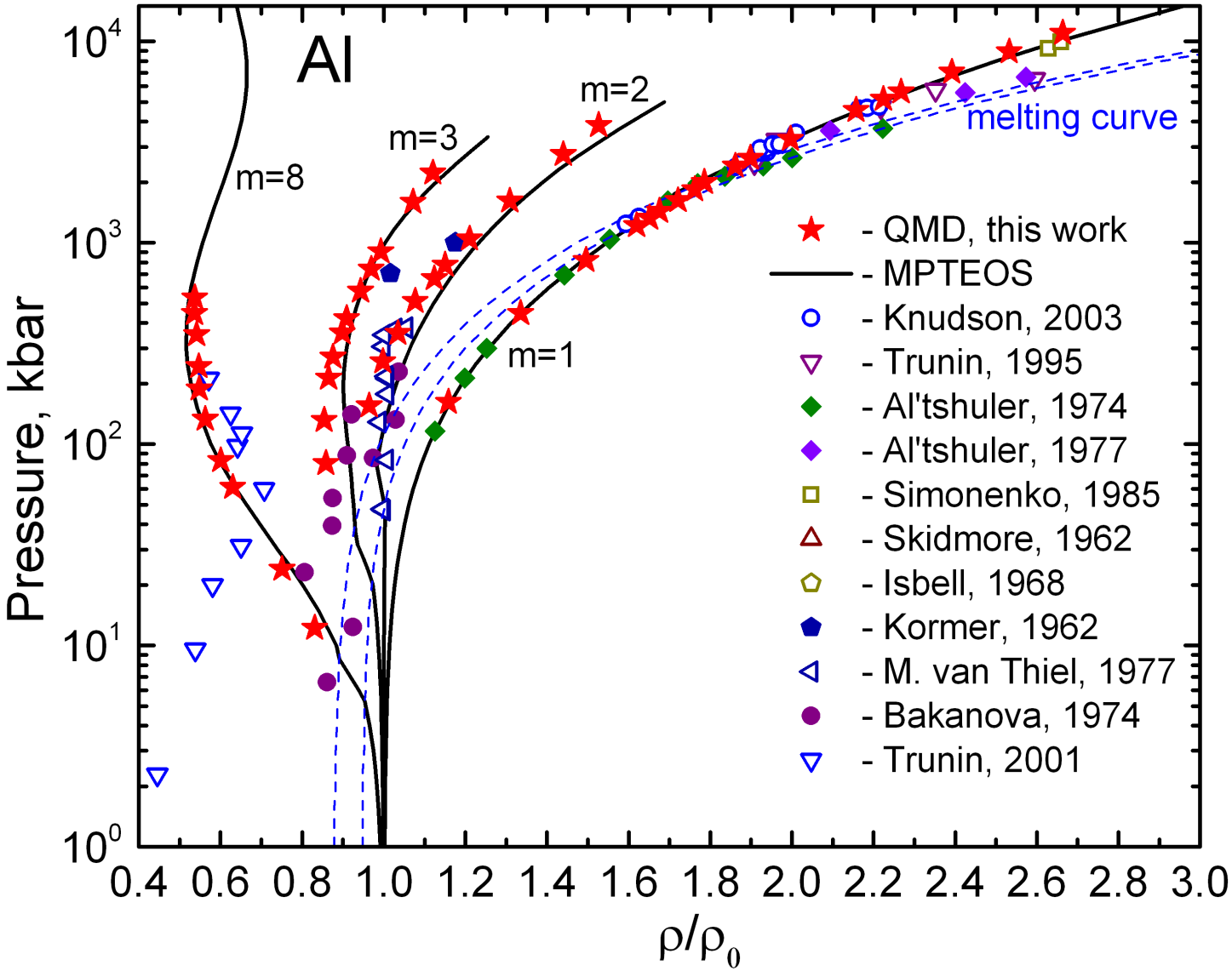

Shock Hugoniot of Al. Melting

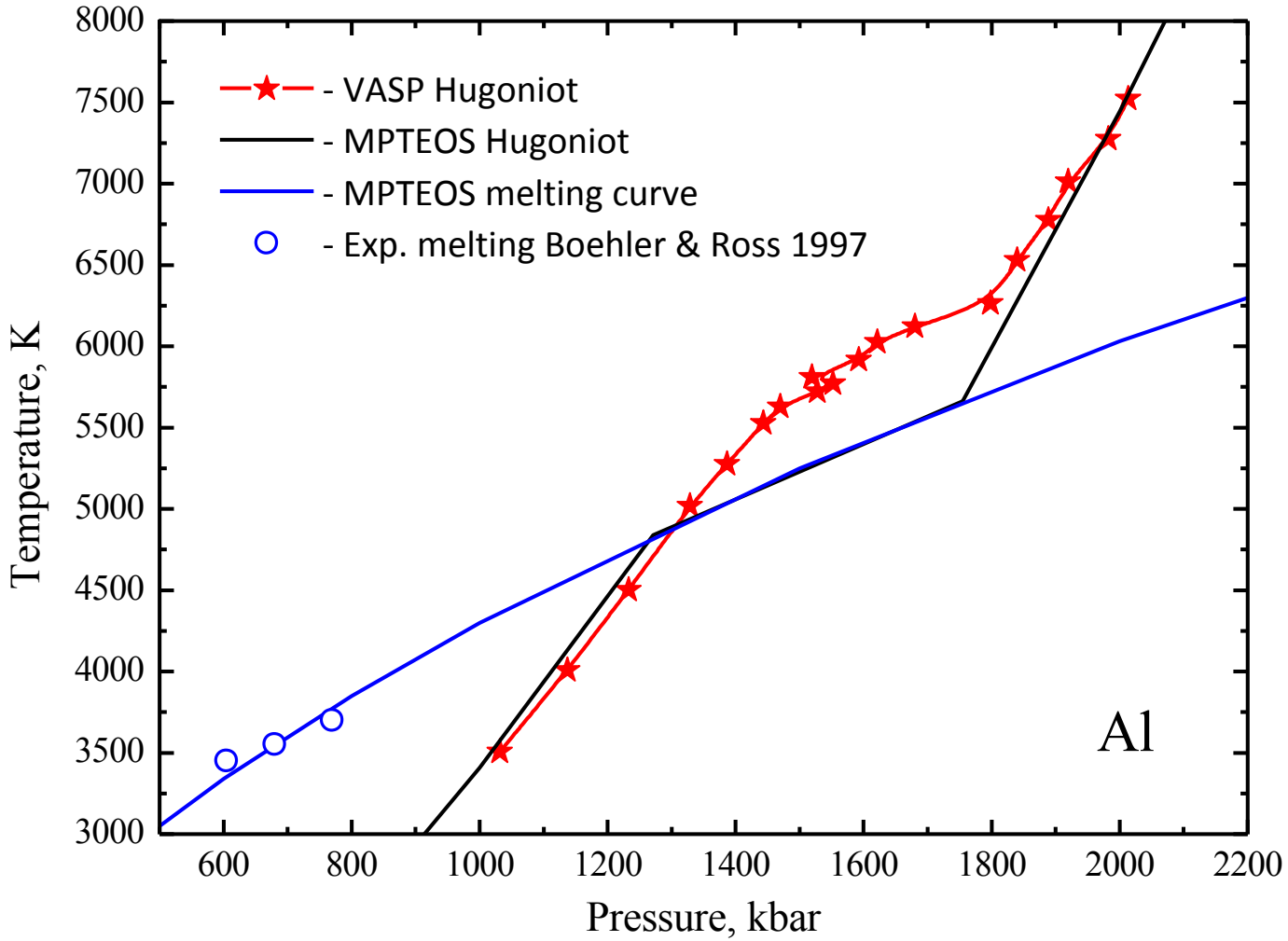

Higher melting temperatures by QMD calculations might be caused by a small number of particles

NB: we can trace phase transitions in 1-phase simulation

Melting criterion for aluminum

Equilibrium configurations of Al ions at 5950 and 6000 K

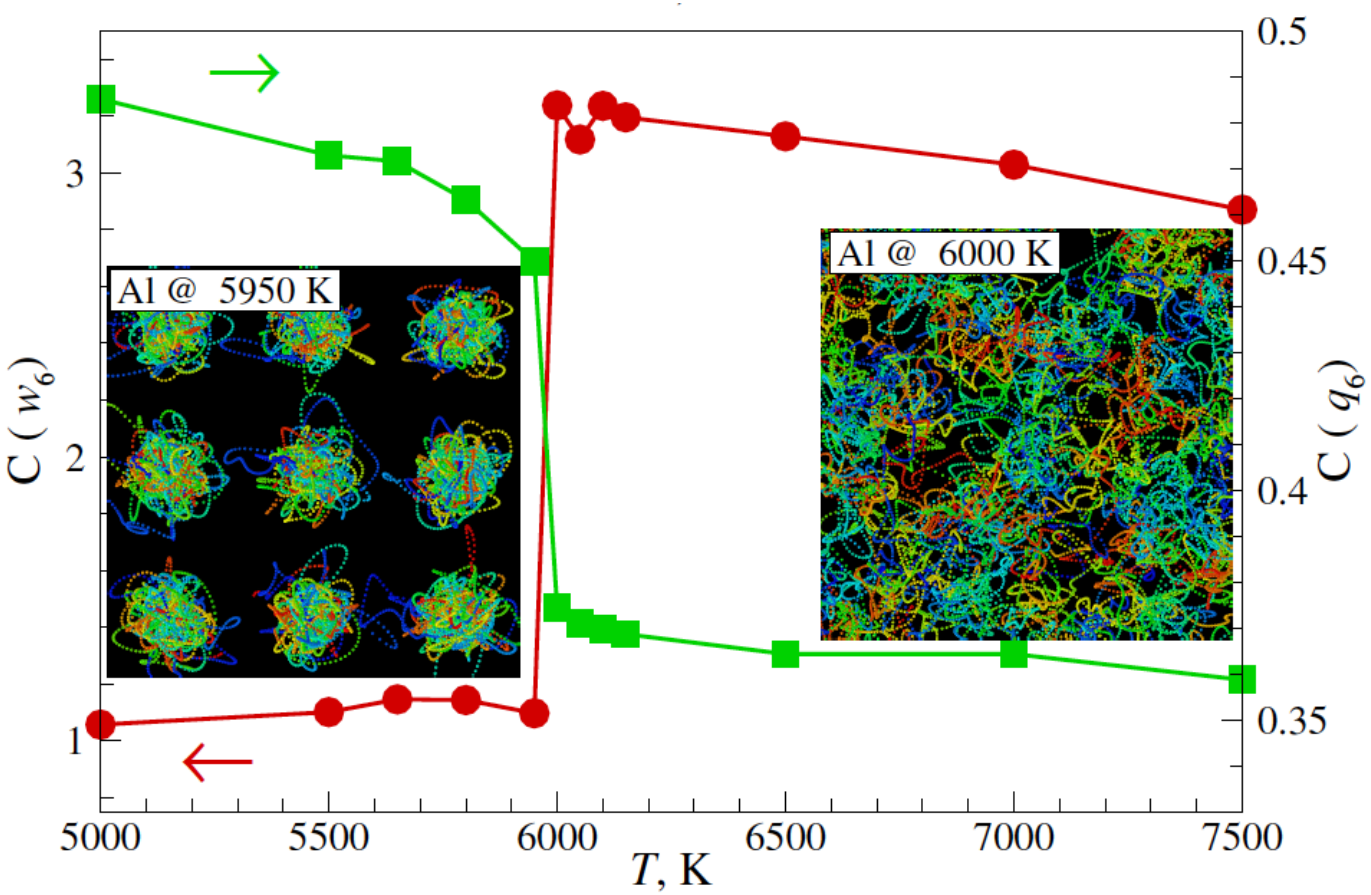

Cumulative distribution functions $C(q_6)$ and $C(w_6)$ are extremely sensitive measure of the local orientation order

This criterion may be applied to other structural phase transitions

Rotational invariants of 2nd (q_6) and 3rd (w_6) orders

$$q_l(i) = \left(\frac{4\pi}{(2l+1)} \sum_{m=-l}^{m=l} | \, q_{lm}(i)|^2 \right)^{1/2}$$

Klumov B.A., Phys. Usp. 53, 1045 (2010)

Steinhardt P.J. et al, PRL 47, 1297 (1981)

Melting curve of aluminum

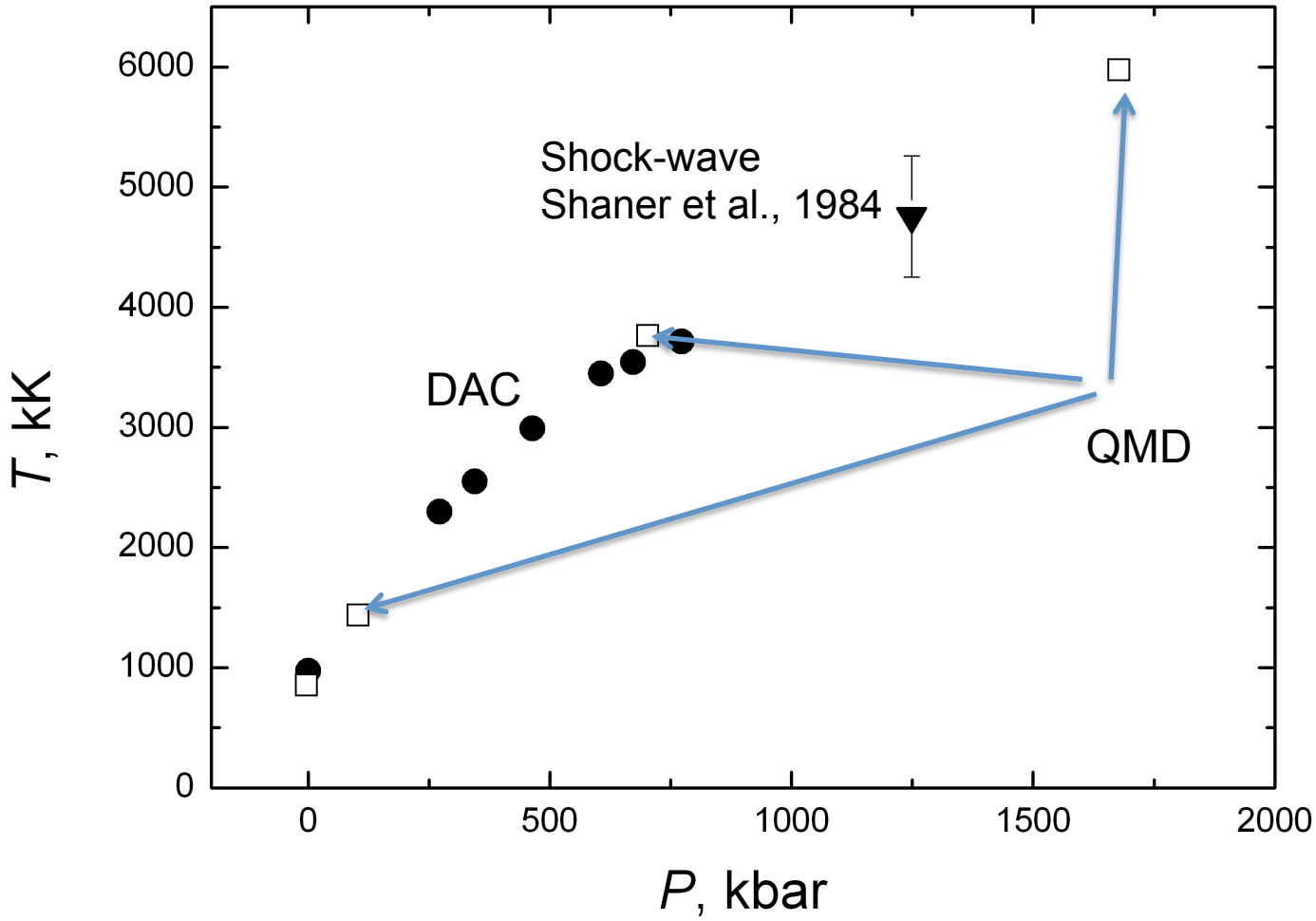

QMD, 108 particles, equilibrium configurations analysis
Size effect should be checked

Boehler R., Ross M. Earth Plan. Sci. Lett. 153, 223 (1997)

Release Isentropes of Al

correspond to the experiments from
M. V. Zhernokletov et al. // Teplofiz. Vys. Temp. 33(1), 40-43 (1995) [in Russian]

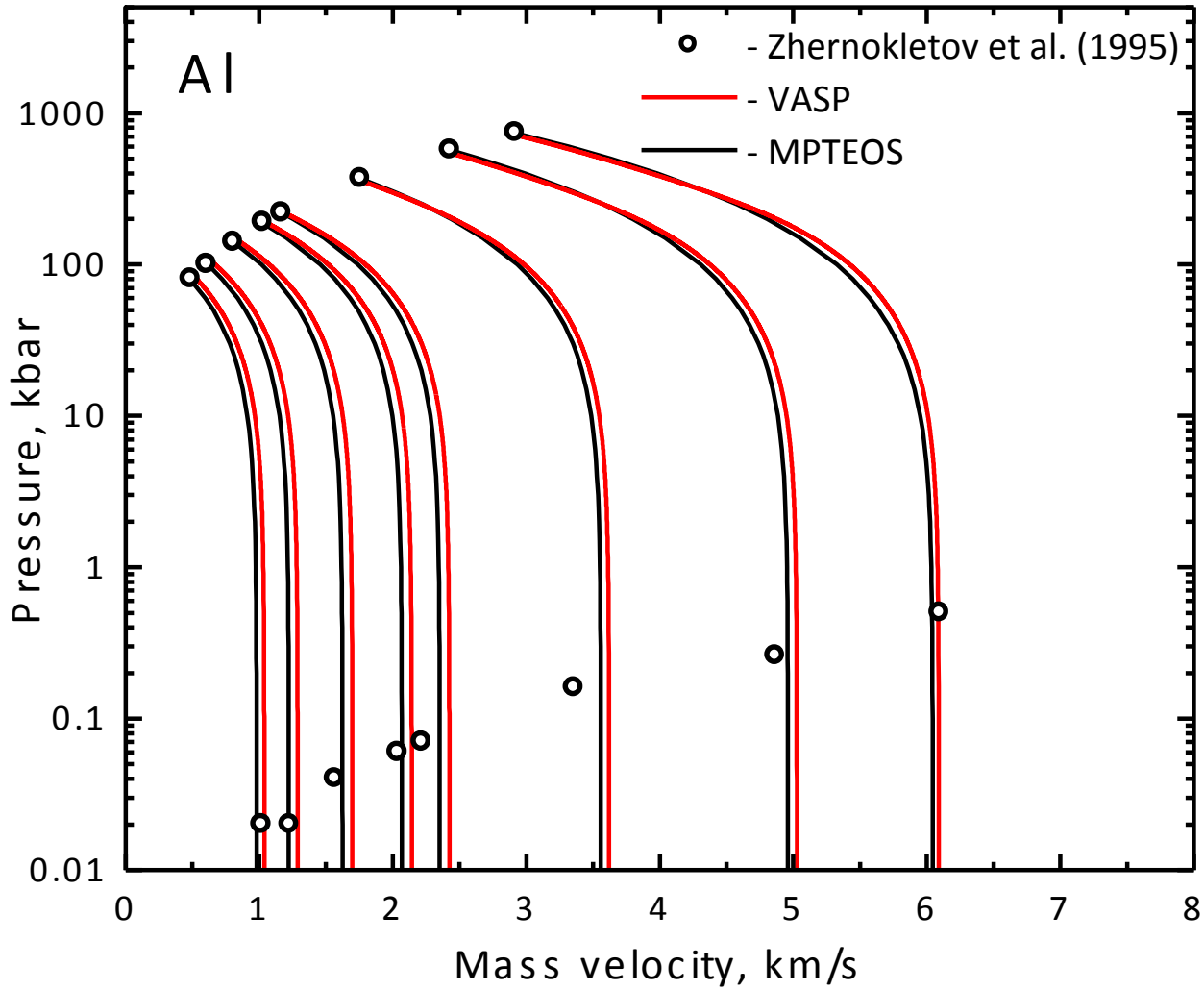

Release Isentropes of Al

correspond to the experiments from

Knudson M.D., Asay J.R., Deeney C. // J. Appl. Phys. V. 97. P. 073514. (2005)

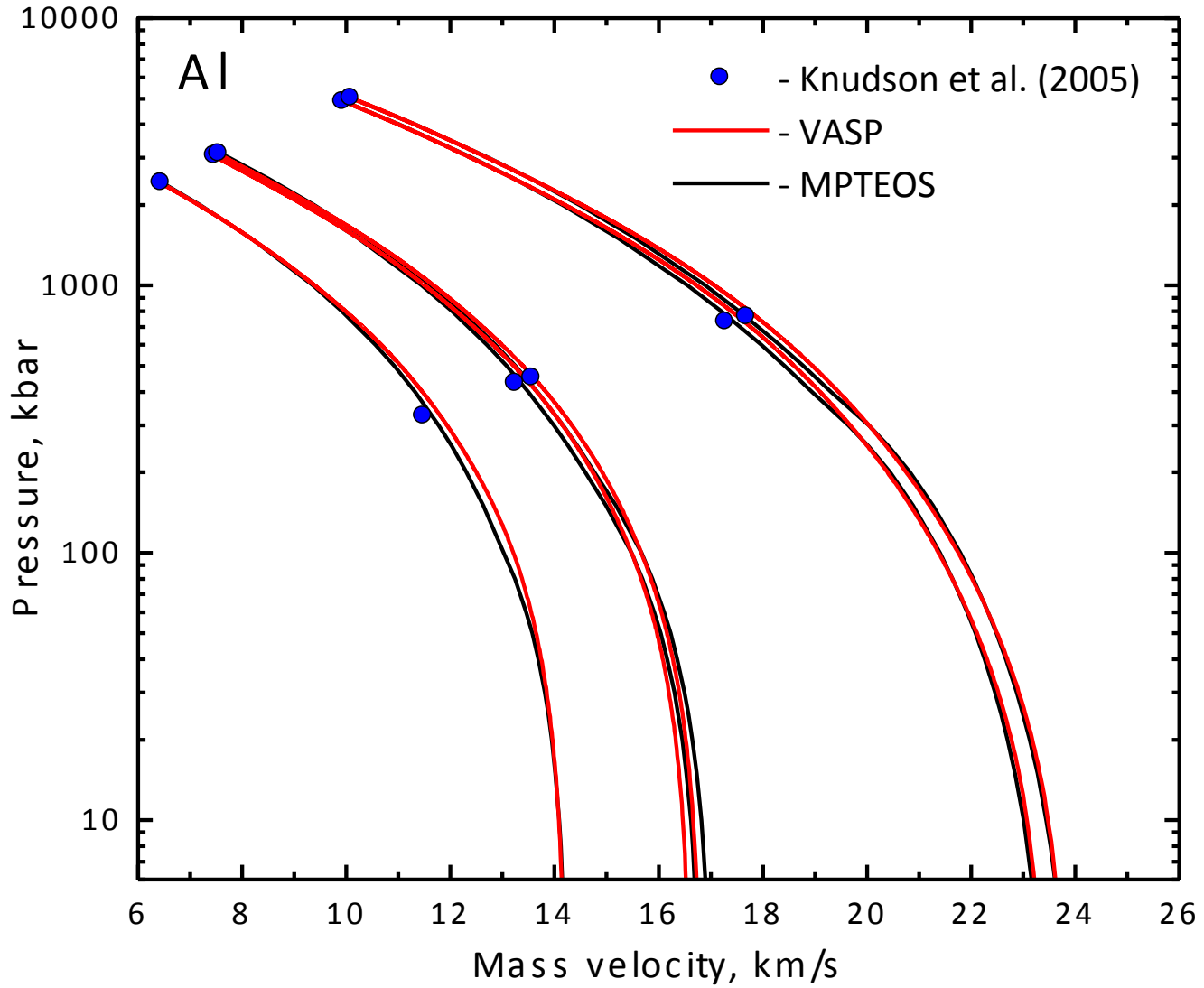

Sound Velocity in Shocked Al

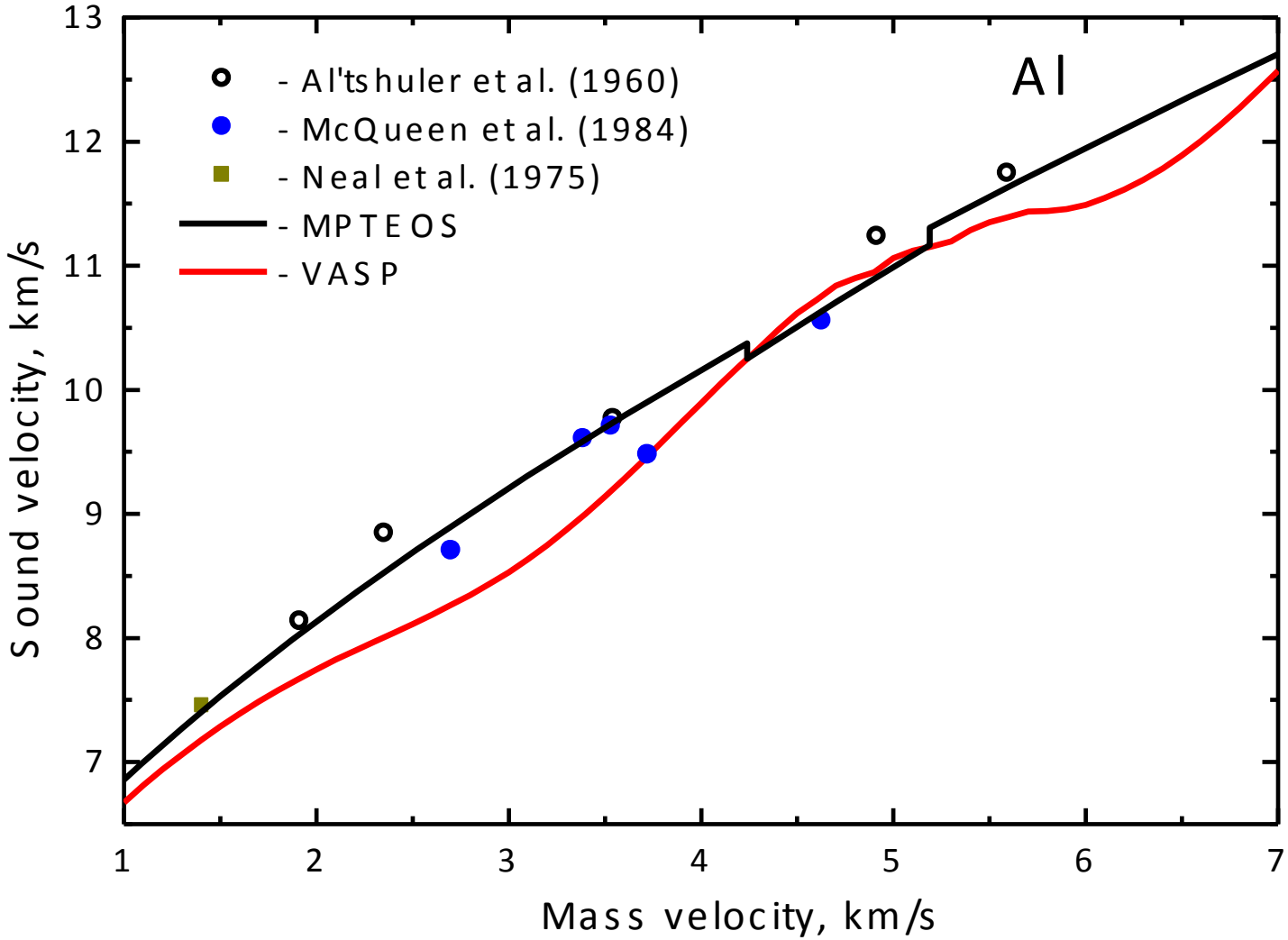

Oscillations are caused by errors of interpolation

Compression Isentrope of Deuterium

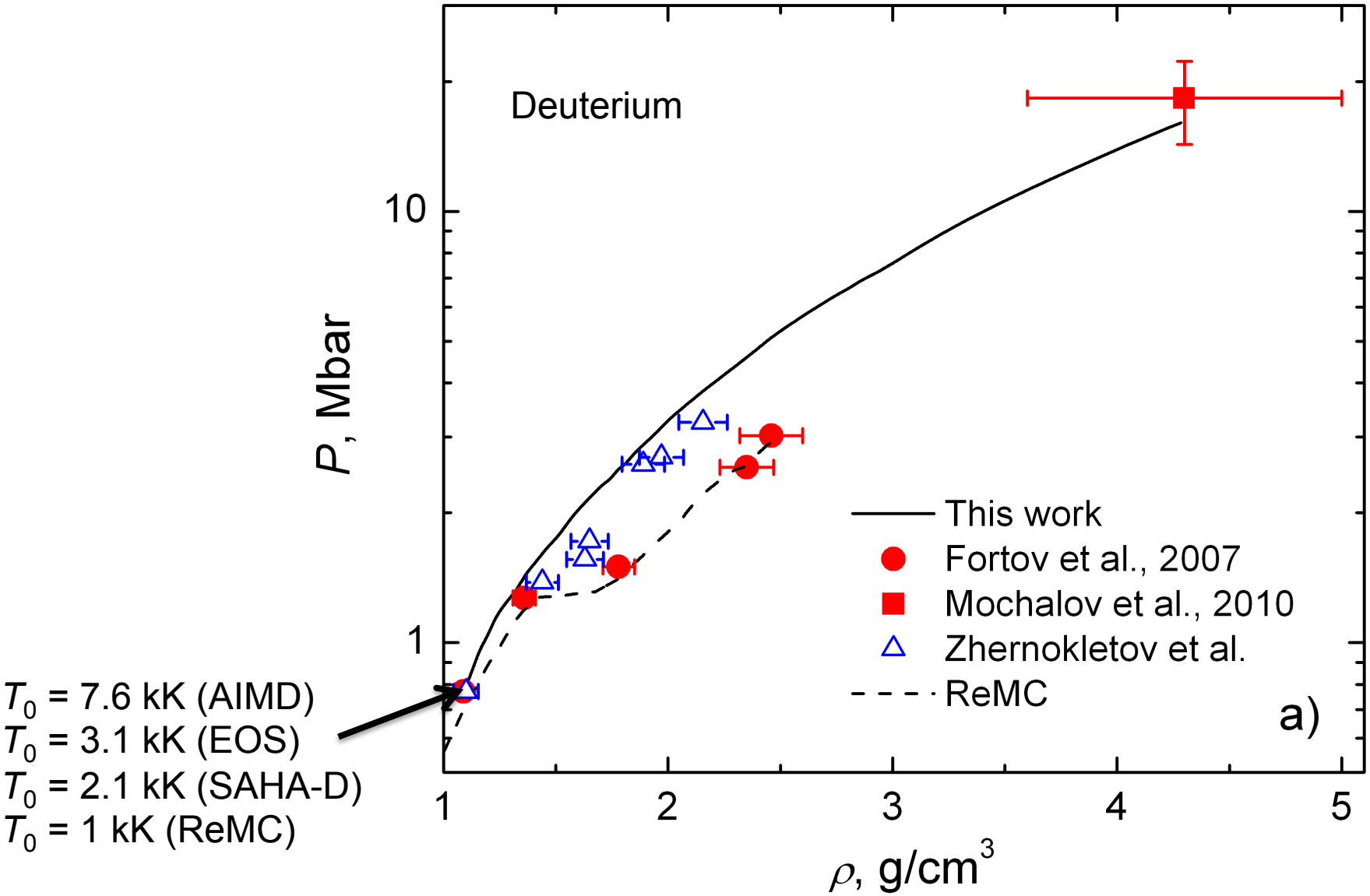

Ab initio complex electrical conductivity

Complex electrical conductivity:

current density

$$\vec{j}_\omega = \left(\sigma_1(\omega) + i\sigma_2(\omega)\right)\vec{E}_\omega$$

electrical field strength

The real part of conductivity is responsible for energy absorption by electrons and is calculated by Kubo-Greenwood formula:

$$\sigma_1(\omega) = \frac{2\pi e^2\hbar^2}{3m^2\omega\Omega}\sum_{i=1}^{N}\sum_{j=1}^{N}\sum_{\alpha=1}^{3}\left[f\left(\varepsilon_i\right) - f\left(\varepsilon_j\right)\right]\left|\left\langle\Psi_j\left|\nabla_\alpha\right|\Psi_i\right\rangle\right|^2\delta\left(\varepsilon_j - \varepsilon_i - \hbar\omega\right)$$

occupancies for the energy level ε

broadening is required

Kubo-Greenwood formula includes matrix elements of the velocity operator, energy levels and occupancies calculated by DFT

The imaginary part of conductivity is calculated by the Kramers-Kronig relation:

$$\sigma_2(\omega) = -\frac{2}{\pi}P\int_0^\infty \frac{\sigma_1(\nu)\omega}{(\nu^2 - \omega^2)}d\nu$$

L.L. Moseley, T. Lukes, Am.J.Phys, **46**, 676 (1978)

Transport properties: Onsager coefficients

Definition of Onsager coefficients L_{mn}:

electric field strength

temperature gradient

current density

$$\vec{j} = \frac{1}{e}\left(L_{11}\vec{E} - \frac{L_{12}\nabla T}{T} \right)$$

heat flow density

$$\vec{j}_q = \frac{1}{e^2}\left(eL_{21}\vec{E} - \frac{L_{22}\nabla T}{T} \right)$$

L_{11} – electrical conductivity

Onsager coefficients are symmetric:

$$L_{12} = L_{21}$$

$$\vec{j}_q = -K\nabla T \quad \text{at} \quad j = 0$$

Using the Onsager coefficients the thermal conductivity coefficient becomes:

$$K = \frac{1}{e^2 T}\left(L_{22} - \frac{L_{12}L_{21}}{L_{11}} \right)$$

thermoelectric term

Wiedemann-Frantz law:

$$\frac{K(T)}{\sigma(T)\cdot T} = L = \frac{\pi^2}{3}\frac{k^2}{e^2}$$

Lorentz number

Optical properties

Imaginary part of electrical conductivity is calculated from the real one by the Kramers-Kronig relation:

$$\sigma_2(\omega) = -\frac{2}{\pi} P \int \frac{\sigma_1(\nu)\omega}{(\nu^2 - \omega^2)} d\nu$$

Real and imaginary parts of complex dielectric function:

$$\varepsilon_1(\omega) = 1 - \frac{\sigma_2(\omega)}{\omega\varepsilon_0}; \varepsilon_2(\omega) = \frac{\sigma_1(\omega)}{\omega\varepsilon_0};$$

Complex index of refraction:

$$n(\omega) = \frac{1}{\sqrt{2}} \sqrt{|\varepsilon(\omega)| + \varepsilon_1(\omega)}; k(\omega) = \frac{1}{\sqrt{2}} \sqrt{|\varepsilon(\omega)| - \varepsilon_1(\omega)};$$

Reflectivity:

$$r(\omega) = \frac{[1 - n(\omega)]^2 + k(\omega)^2}{[1 + n(\omega)]^2 + k(\omega)^2}$$

Static electric conductivity is calculated by linear extrapolation (by 2 points) of dynamic electrical conductivity to zero frequency

Al, T=1550 K, ρ=2.23 g/cm^3

Real part of electrical conductivity

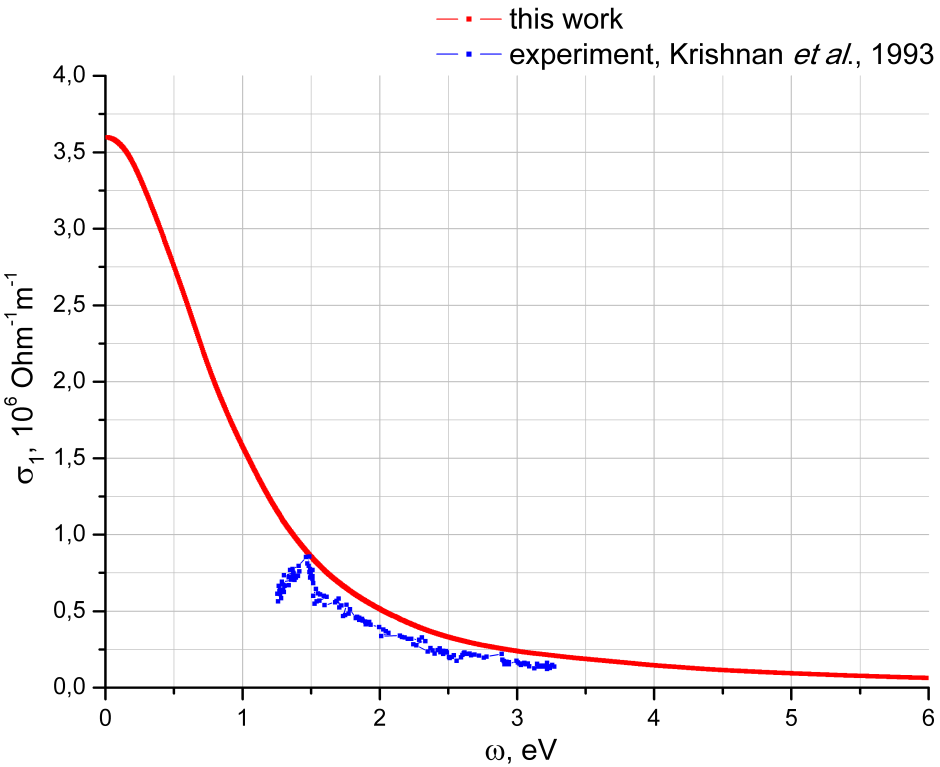

Real part of dielectric function

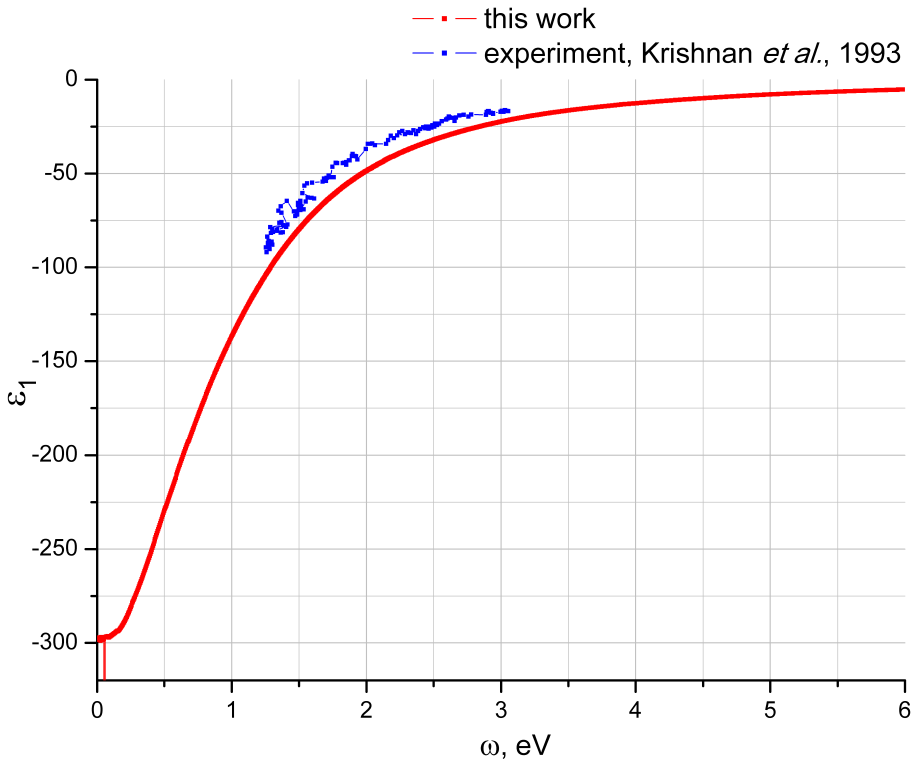

256 atoms; US pseudopotential; 1 k-point in the Brillouine zone; cut-off energy 200 eV;
δ-function broadening 0.1 eV; 15 configurations; 1500 steps; 1 step – 2 fs

In liquid phase the dependence of electrical conductivity is Drude-like.
The agreement with reference data is good

Krishnan et al., Phys. Rev. B, **47**, 11 780 (1993)

Al, 1000 K – 10000 K, ρ = 2.35 g/cm^3

Static electrical conductivity

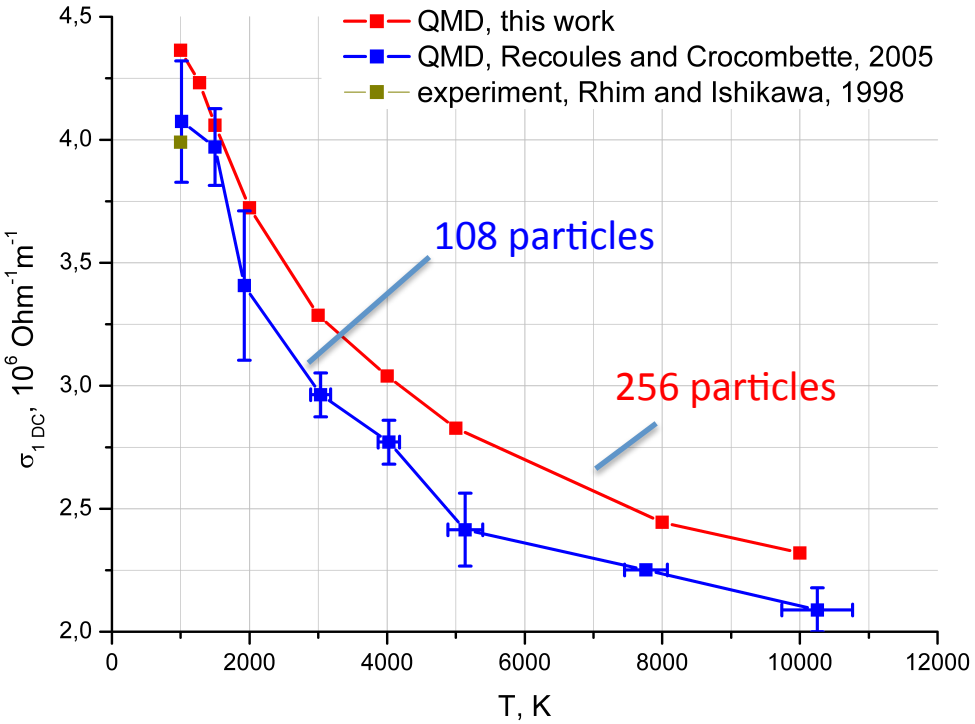

Thermal conductivity coefficient

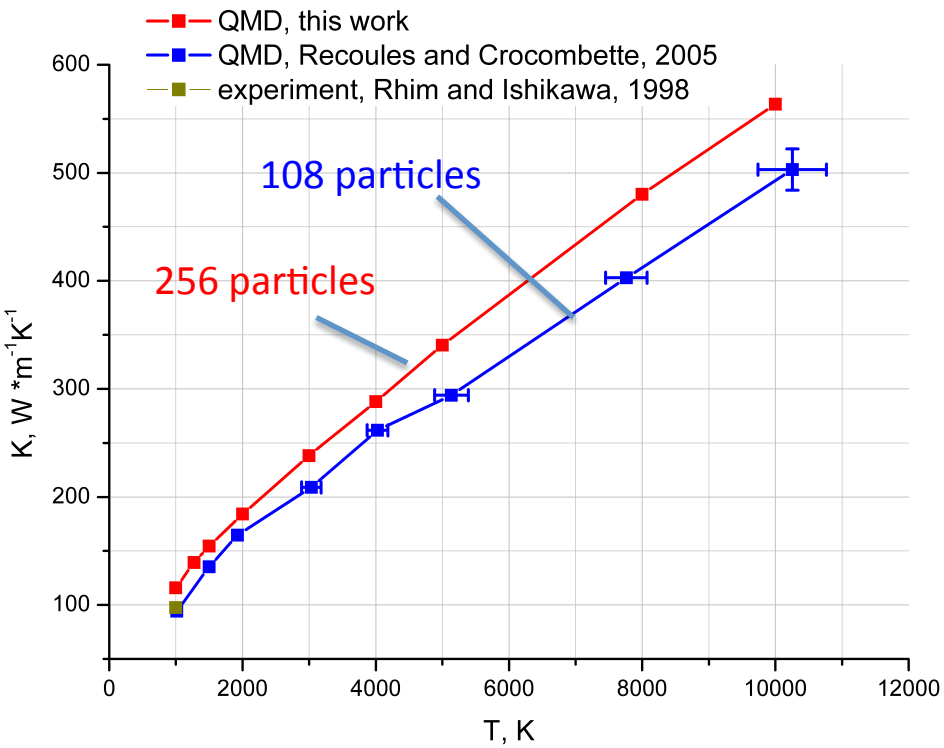

256 atmos; US pseudopotential; 1 k-point in the Brillouin zone; energy cut-off 200 eV; δ-function broadening 0.07 eV - 0.1 eV ; 15 configurations; 1500 steps; 1 step – 2 fs

Thermoelectric correction is not more than 2% at $T < 10$ kK

Recoules and Crocombette, Phys. Rev. B, **72**, 104202 (2005)
Rhim and Ishikawa, Rev. Sci. Instrum., **69**, 10, 3628-3633 (1998)

Al, 1000 K – 20000 K, 2.35-2.70 g/cm^3

Dependence of Lorentz number on temperature

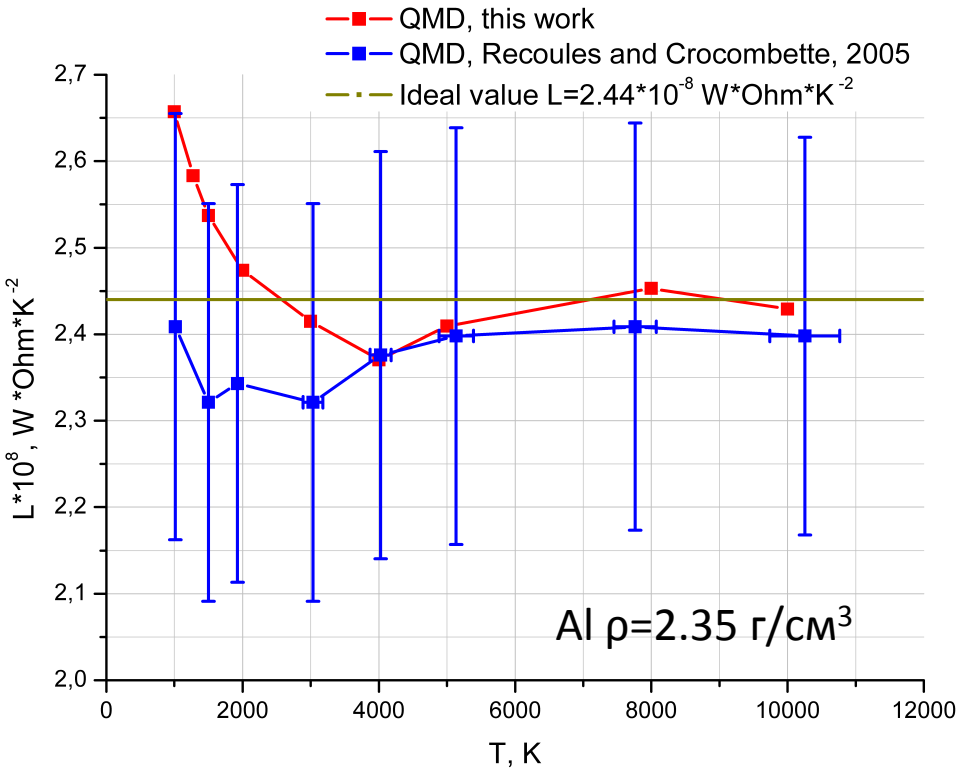

Thermal conductivity and Onsager $\mathcal{L}_{22}$ coefficient, temperature dependence

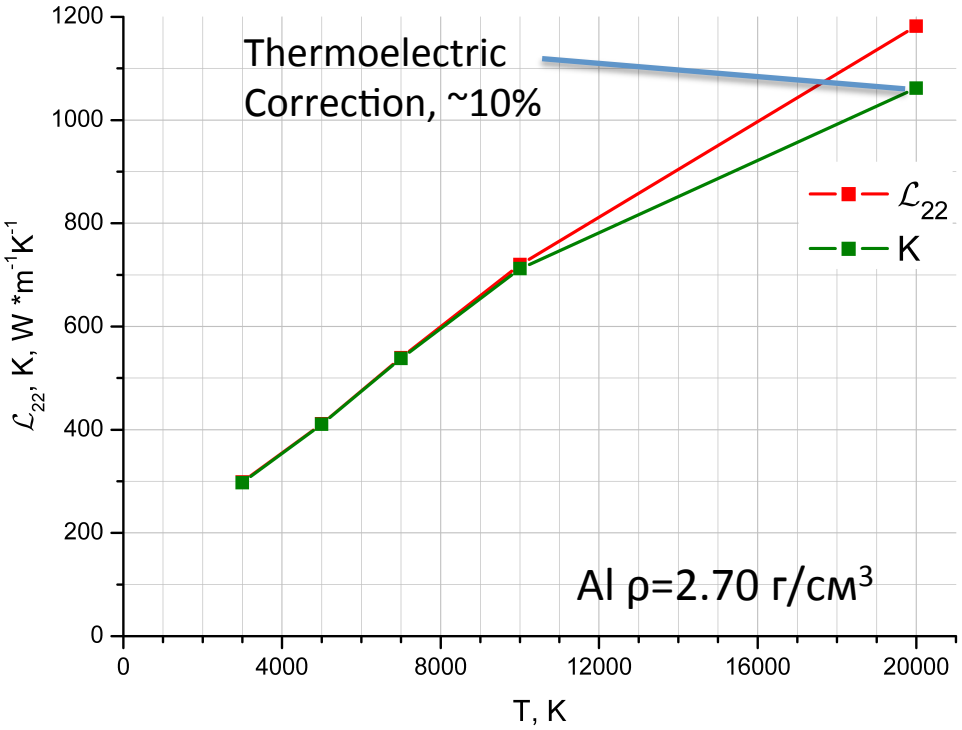

256 atoms; US pseudopotential; 1 k-point in the Brillouin zone; energy cut-off 200 eV; δ-function broadening 0.07 eV - 0.1 eV; 15 configurations; 1500 steps; 1 step – 2 fs

Distinction of Lorentz number from the ideal value is about 20%.
Thermoelectric correction is substantial only at 20 kK (10%).

Recoules and Crocombette, Phys. Rev. B, **72**, 104202 (2005)

Beyond DFT and Mean Atom: Path Integral Monte Carlo and Wigner Dynamics

PATH INTEGRAL MONTE-CARLO METHOD

for degenerate hydrogen plasma

(V. M. Zamalin, G. E. Norman, V. S. Filinov, 1973-1977)

- Binary mixture of N_e quantum electrons,
  N_i classical protons

- Partition function:

$$Z(N_e,N_i,V,\beta)=Q(N_e,N_i,\beta)/N_e!N_i!$$

$$Q(N_e,N_i,\beta)=\sum_{\sigma}\int_{V} dq\,dr\,\rho(q,r,\sigma;\beta)$$

- Density matrix:

$$\rho=\exp(-\beta H)=\exp(-\Delta\beta H)\times\ldots\times\exp(-\Delta\beta H)$$

$n+1$

$$\beta=1/kT \qquad \Delta\beta=\beta/(n+1)$$

PATH INTEGRAL MONTE-CARLO METHOD

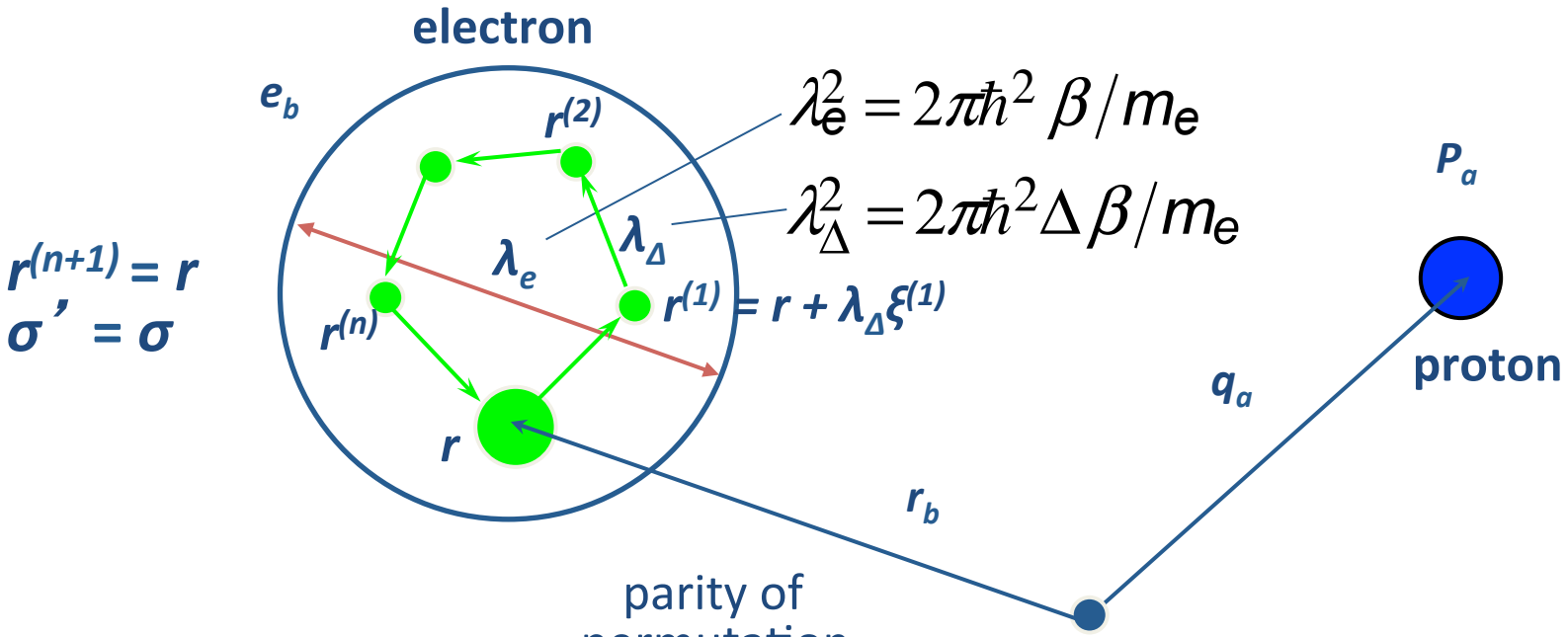

parity of permutation

$$\rho(q,r,\sigma;\beta) = \frac{1}{\lambda_i^{3N_i}\,\lambda_\Delta^{3N_e}} \sum_P (-1)^{\kappa_P} \int_V dr^{(1)} \ldots dr^{(n)} \times$$

$$\rho\left(q,r,r^{(1)};\Delta\beta\right)\ldots\rho\left(q,r^{(n)},Pr^{(n+1)};\Delta\beta\right)S\left(\sigma,P\sigma'\right),$$

thermal wavelengths of electron and ion

permutation operator

spin matrix

PATH INTEGRAL MONTE-CARLO METHOD

Path integral representation of density matrix:

$$\rho(q,r,\sigma;\beta)=\int_V dR^{(1)}\ldots dR^{(n)}\,\rho^{(1)}\ldots\rho^{(n)}\sum_P(-1)^{k_P}\,S\left(\sigma,\hat{P}\sigma'\right)\hat{P}\rho^{(n+1)}$$

$$R^{(i)}=\left(q^{(i)},r^{(i)}\right)$$

$$\rho^{(i)}=\left\langle R^{(i-1)}\left|e^{-\Delta\beta\hat{H}}\right|R^{(i)}\right\rangle$$

spin matrix

permutation operator

$$\hat{H}=\hat{K}+\hat{U}_c,\quad \hat{U}_c=\hat{U}_c^p+\hat{U}_c^e+\hat{U}_c^{ep}$$

$$\sum_\sigma\rho(q,r,\sigma;\beta)=\left(\prod_{l=1}^{n}e^{-\Delta\beta U_l(\Delta\beta)}\prod_{p=1}^{N_e}\phi_{pp}^{l}\right)\sum_{s=0}^{N_e}C_{N_e}^{s}\det\left\|\psi_{ab}^{n,1}\right\|_s$$

$$U_l^p(\Delta\beta)+U_l^e(\Delta\beta)+U_l^{ep}(\Delta\beta)$$

kinetic part of density matrix

exchange effects

KELBG PSEUDOPOTENTIAL

First order perturbation theory solution of two-particle Bloch equation for density matrix in the limit of weak coupling

$$\Phi^{ab}(\mathbf{r}_{ab},\mathbf{r}'_{ab},\Delta\beta)=e_a e_b\int_0^1\frac{d\alpha}{d_{ab}(\alpha)}\operatorname{erf}\left(\frac{d_{ab}(\alpha)}{2\lambda_{ab}\sqrt{\alpha(1-\alpha)}}\right)$$

$$d_{ab}(\alpha)=\left|\alpha\mathbf{r}_{ab}+(1-\alpha)\mathbf{r}'_{ab}\right|$$

$$\lambda_{ab}=\hbar^2\beta/2\mu_{ab}$$

$$\mu_{ab}^{-1}=m_a^{-1}+m_b^{-1}$$

Diagonal Kelbg potential:

$$\Phi^{ab}(\mathbf{r}_{ab},\Delta\beta)=\frac{e_a e_b}{\lambda_{ab}x_{ab}}\left\{1-e^{-x_{ab}^2}+\sqrt{\pi}x_{ab}\left[1-\operatorname{erf}(x_{ab})\right]\right\}$$

$$x_{ab}=\left|\mathbf{r}_{ab}\right|/\lambda_{ab}$$

$$\left|\mathbf{r}_{ab}\right|\to 0:\quad\frac{\sqrt{\pi}e_a e_b}{\lambda_{ab}}$$

$$\left|\mathbf{r}_{ab}\right|>>\lambda_{ab}:\quad\frac{e_a e_b}{|r_{ab}|}$$

Ebeling et al., Contr. Plasma Phys., 1967

ACCURACY OF DIRECT PIMC

$$\hat{\rho} = e^{-\beta \hat{H}} = \underbrace{e^{-\Delta\beta\hat{H}} \times \ldots \times e^{-\Delta\beta\hat{H}}}_{n+1}$$

$$\beta = 1/k_B T \qquad \hat{H} = \hat{K} + \hat{U}$$

$$\Delta\beta = \beta/(n+1)$$

$$\hat{\rho}_{\Delta\beta} = e^{-\Delta\beta\hat{H}} = e^{-\Delta\beta\hat{K}} e^{-\Delta\beta\hat{U}} e^{-\frac{(\Delta\beta)^2}{2}[\hat{K},\hat{U}]}$$

1 at $n \to \infty$

Error ~ $(\beta / n)^2$ for every multiplier

Total error $\Delta\rho \sim \beta^2 / n \to 0$ at $n \to \infty$

$$\rho_{\Delta\beta} = \rho_{free} \rho_{pot}(\Delta\beta)$$

High-temperature pseudopotential

TREATMENT OF EXCHANGE EFFECTS

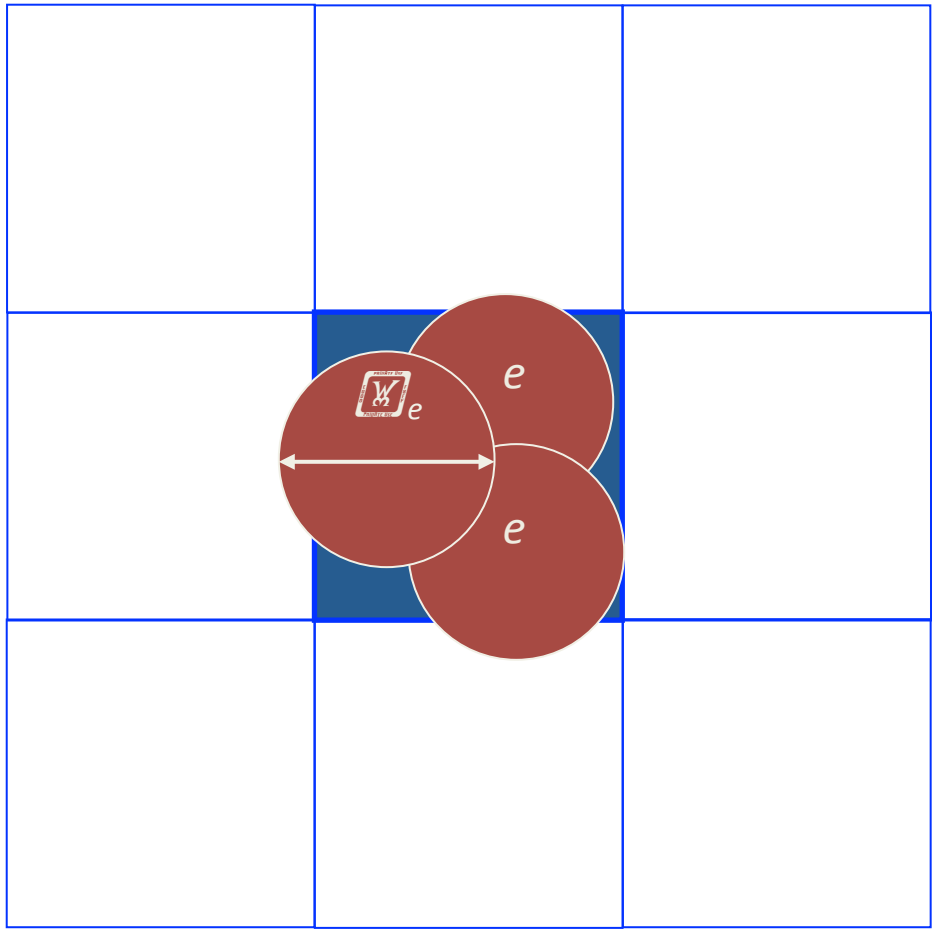

Inside main cell –
exchange matrix

Outside main cell –
by perturbation theory

Accuracy control –
comparison with ideal
degenerate gas

$$n_e \lambda_e^3 \sim 300$$

Filinov V.S. // J. Phys. A: Math. Gen. ***34****, 1665 (2001)*
Filinov V.S. et al. // J. Phys. A: Math. Gen. ***36****, 6069 (2003)*

HYDROGEN, PIMC-SIMULATION, $n = 10^{21}$ cm^{-3}

$N_e = N_i = 56$, $n = 20$

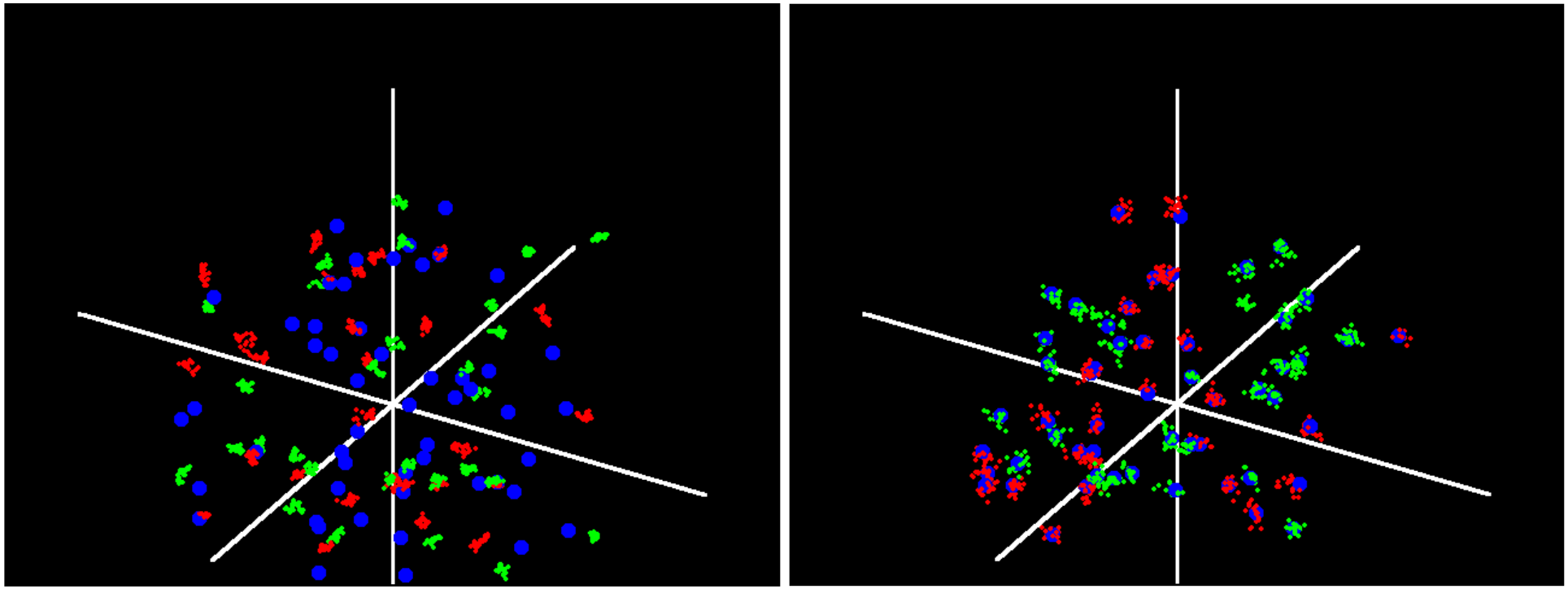

$T = 50$ kK

$\rho = 1.67 \times 10^{-3}$ g/cm^3

$\Gamma = 0.54$

$n\lambda^3 = 3.7 \times 10^{-2}$

$T = 10$ kK

$\Gamma = 2.7$

$n\lambda^3 = 0.41$

- proton
- electron
- electron

HYDROGEN, PIMC-SIMULATION AND CHEMICAL PICTURE, $n_e = 10^{20}, 10^{21}$ cm^{-3}

Pressure

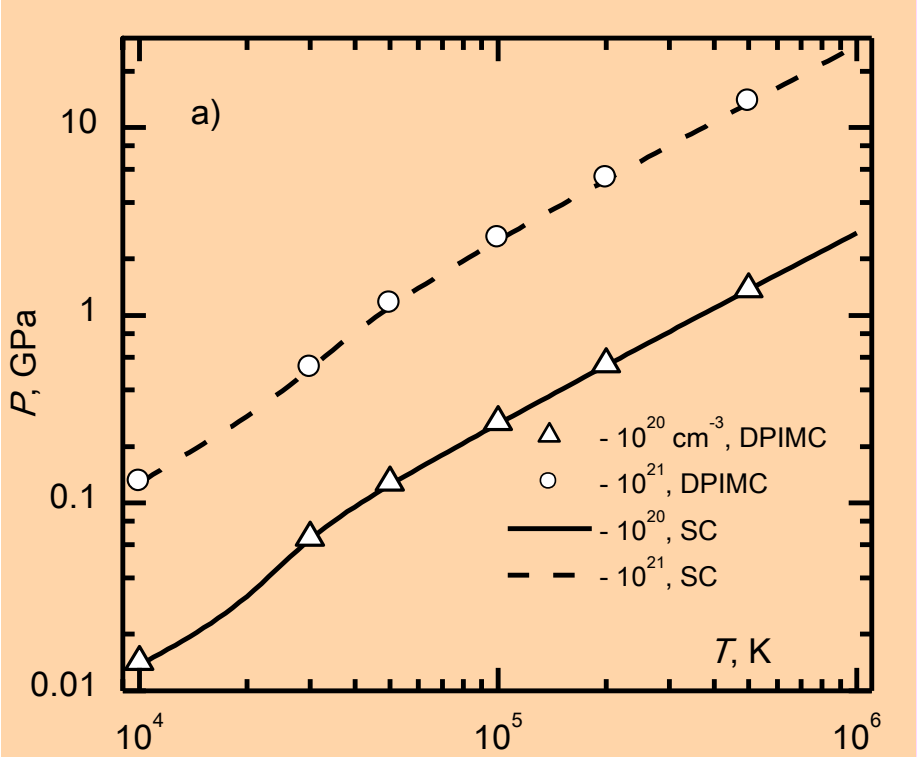

Energy

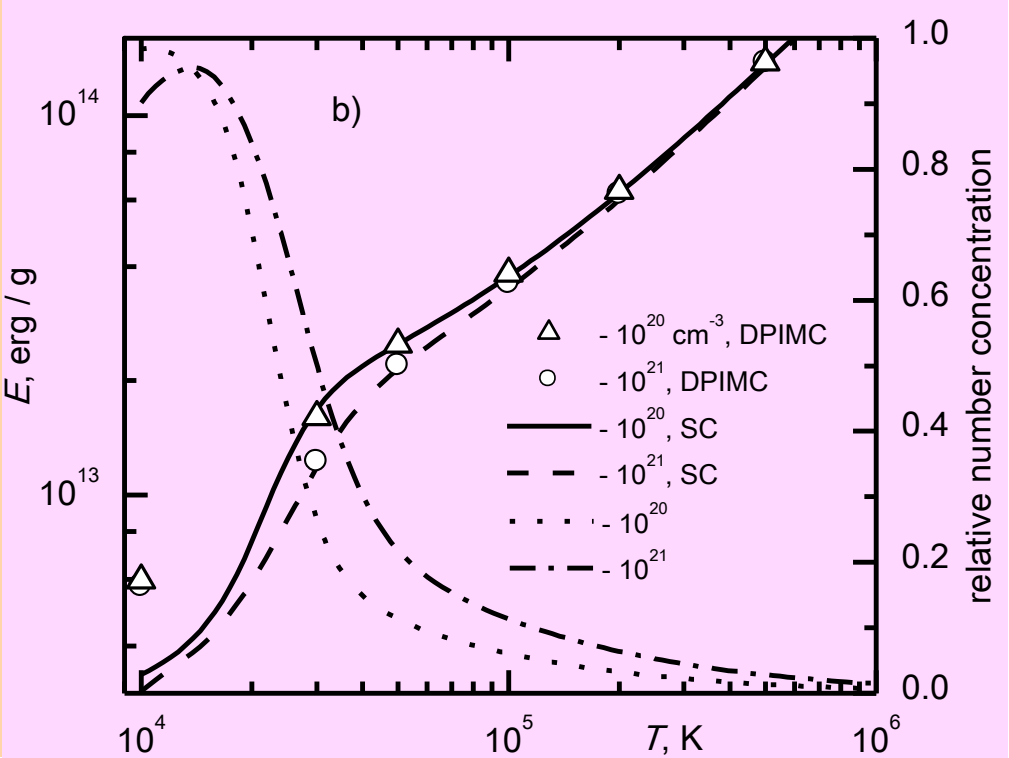

D. Saumon, G. Chabrier, H.M. Van Horn, Astrophys. J. Suppl.Ser. 1995. V.99. P.713

DEUTERIUM SHOCK HUGONIOTS

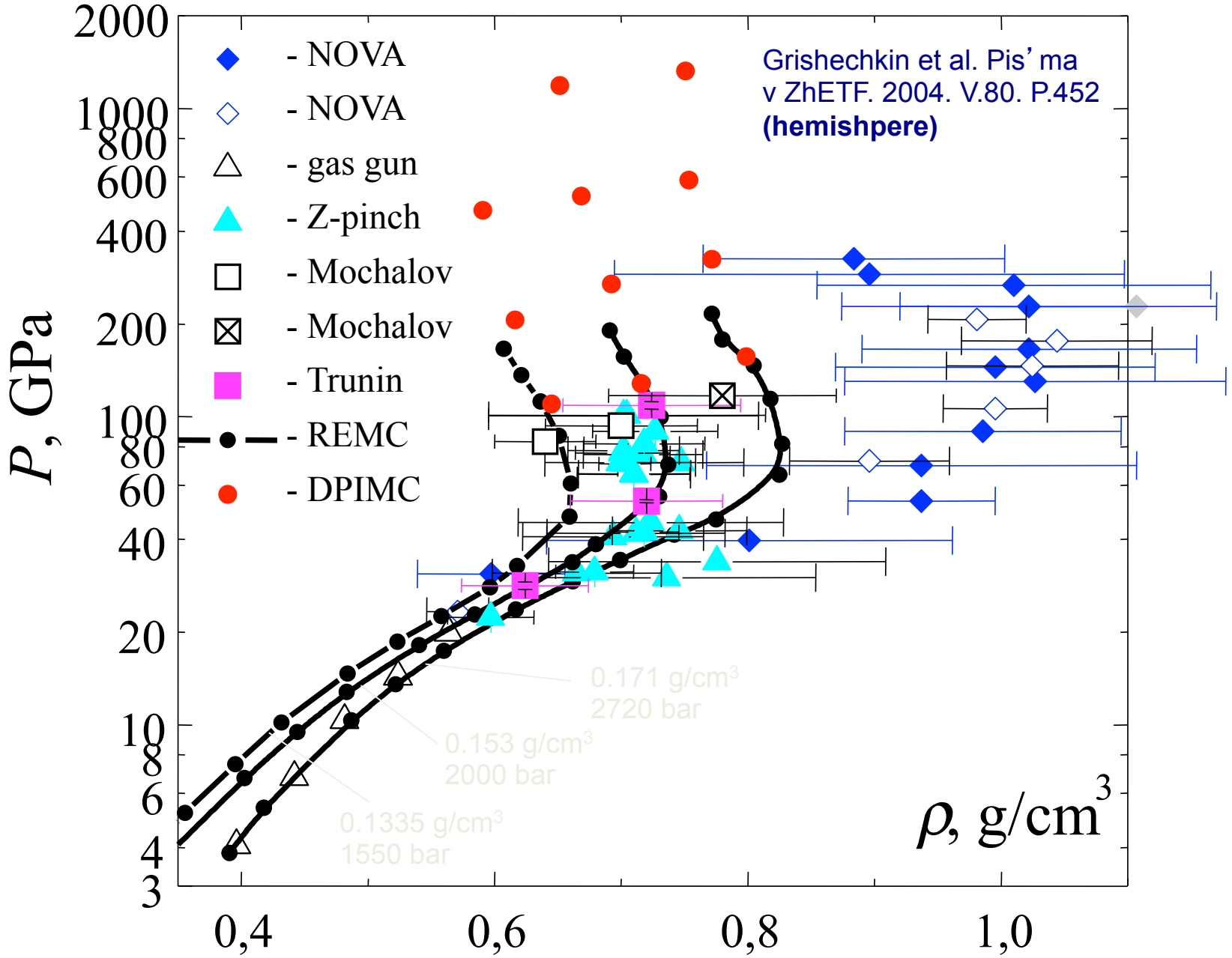

HYDROGEN, PIMC-SIMULATION, T = 10000 K

$N_e = N_i = 56$, $n = 20$

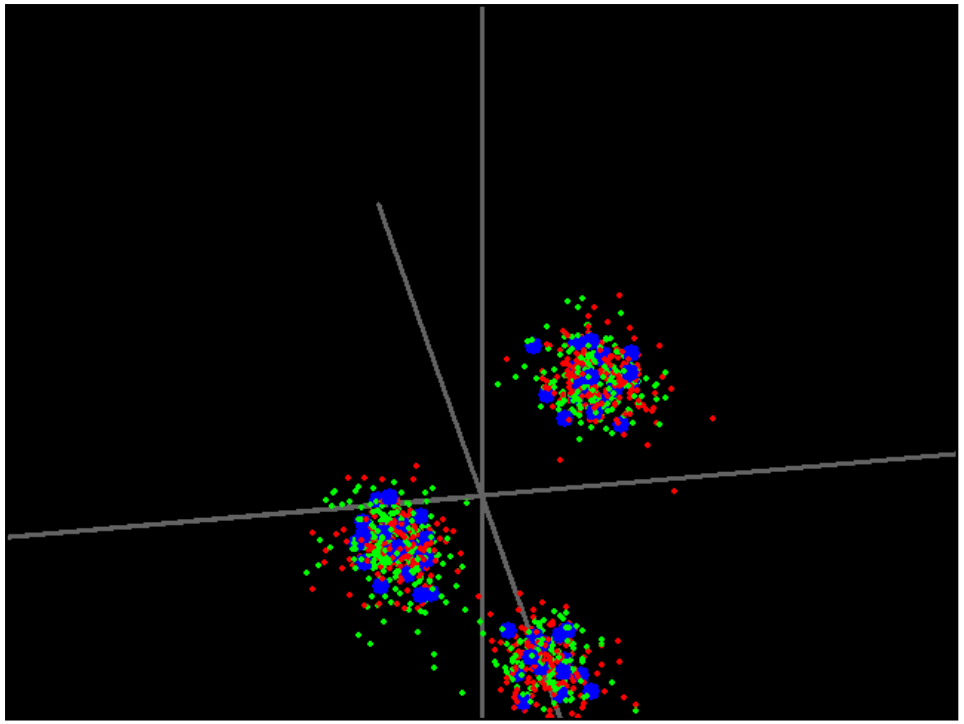

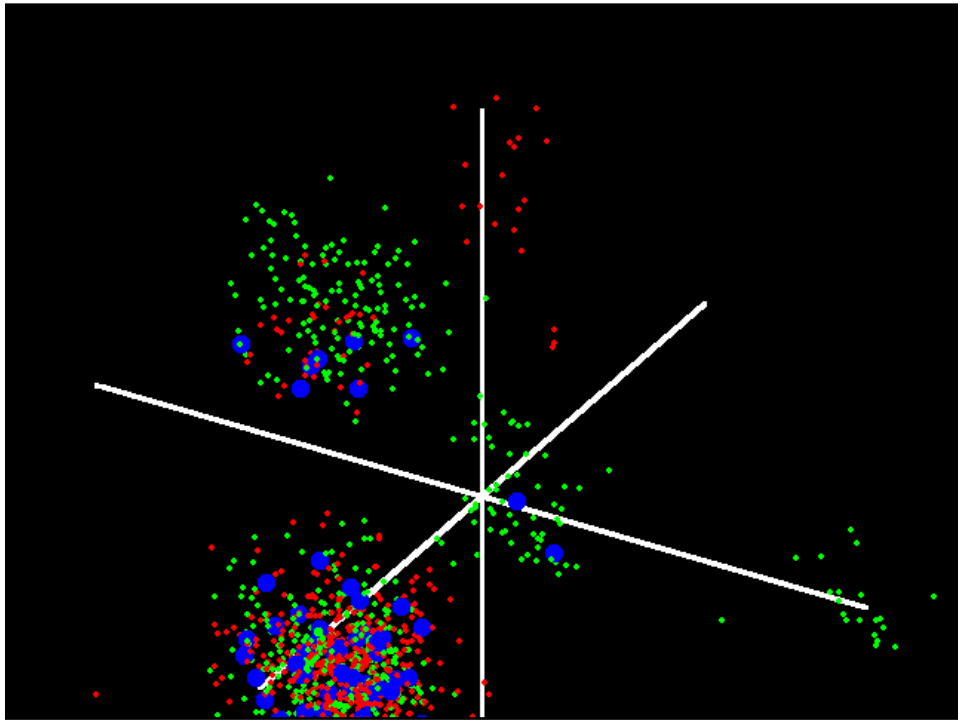

$n = 3 \times 10^{22}$ cm^{-3}
$\rho = 0.05$ g/cm^3
$\Gamma = 8.4$
$n\lambda^3 = 12.4$

$n = 10^{23}$ cm^{-3}
$\rho = 0.167$ g/cm^3
$\Gamma = 12.5$
$n\lambda^3 = 41$

- proton
- electron
- electron

PIMC SIMULATION

$N_e = N_i = 56$, $n = 20$
protons ordering

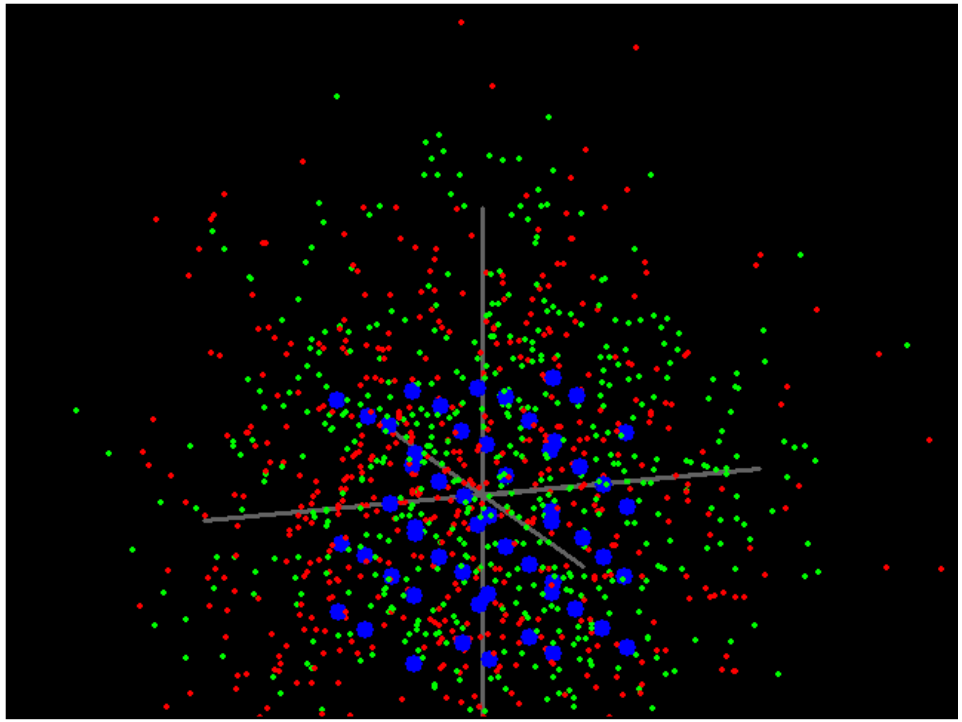

- proton
- electron
- electron

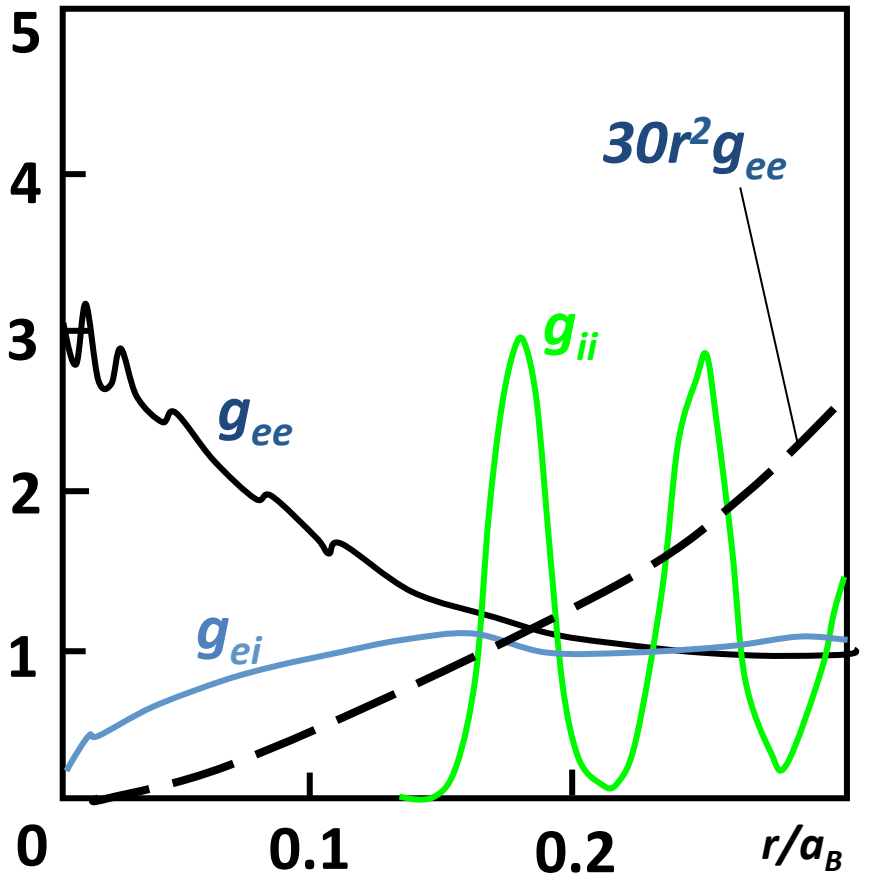

$T = 10000$ K,
$n = 3 \times 10^{25}$ cm^{-3},
$\rho = 50.2$ g/cm^3
$\Gamma = 84$
$n\lambda^3 = 12400$

JETP Letters **72**, 245 (2000)

ELECTRON DENSITY DISTRIBUTION IN TWO-COMPONENT DEGENERATE SYSTEM

IN COULOMB CRYSTAL

$m_h = 800$ $\rho = 25$

$m_e = 2.1$ $T / E_b = 0.002$

$\langle r \rangle / a_B = 3$

- hole
- hole
- electron
- electron

top view

side view

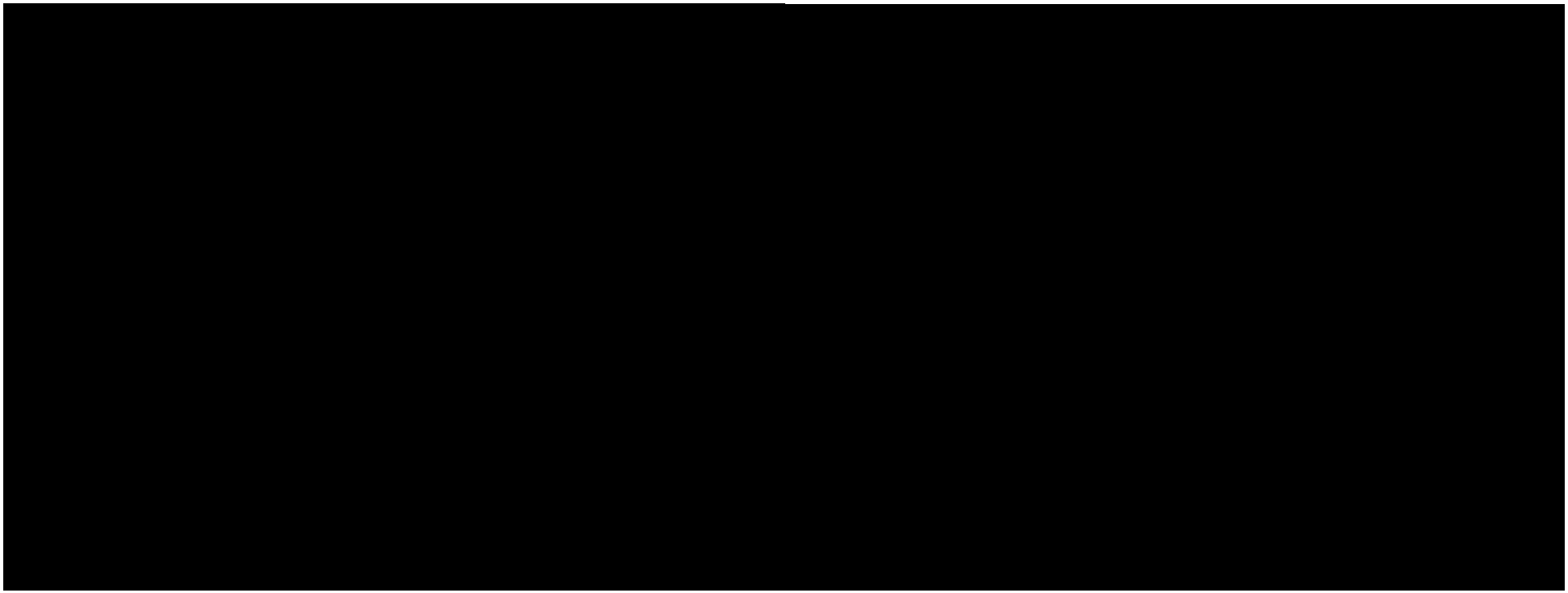

QUANTUM DYNAMICS IN WIGNER REPRESENTATION

Quasi-distribution function in phase space for the quantum case

Density matrix: $\rho(q',q'') = \psi^*(q')\psi(q'') \qquad \psi \in C \qquad i\frac{\partial \rho}{\partial t} = [\hat{H}, \rho]$

Wigner function: $W^L(q,p) = \frac{1}{(2\pi)^{Nd}} \int \rho\left(q + \frac{\xi}{2}, q - \frac{\xi}{2}\right) e^{-ip\xi} d\xi$

$$\rho(q',q'') = \int W^L\left(\frac{q'+q''}{2}, p\right) e^{i(q'-q'')p} dp \qquad W^L \in R$$

Evolution equation: $\frac{\partial W^L}{\partial t} + \left\langle \frac{p}{m} \middle| \frac{\partial W^L}{\partial q} \right\rangle = \int ds W^L(p-s,q,t)\omega(s,q)ds$

$$\omega(s,q) = \frac{2}{(2\pi)^{Nd}} \int dq' U(q-q') \sin\left[\frac{2sq'}{\hbar}\right]$$

Classical limit $\hbar \to 0$:

$$\frac{\partial W^L}{\partial t} + \left\langle \frac{p}{m} \middle| \frac{\partial W^L}{\partial q} \right\rangle - \left\langle \frac{\partial U}{\partial q} \middle| \frac{\partial W^L}{\partial p} \right\rangle = 0$$

Characteristics (Hamilton equations):

$$\langle \dot{q} | = \left\langle \frac{p}{m} \right| \qquad \langle \dot{p} | = -\left\langle \frac{\partial U}{\partial q} \right|$$

SOLUTION OF WIGNER EQUATION

$$W(p,q,t) = \int \Pi^W(p,q,t;p_0,q_0,0) \times W_0(p_0,q_0) dp_0 dq_0 +$$

$$\int_0^t d\tau' \int\int dp_{\tau'} dq_{\tau'} \Pi^W(p,q,t;p_{\tau'},q_{\tau'},\tau') \times \int_{-\infty}^{\infty} ds W(p_{\tau'} - s, q_{\tau'}, \tau') \omega(s, q_{\tau'})$$

Dynamical trajectories:

$$\frac{d\bar{p}}{dt} = F(\bar{q}(t)), \; \bar{q}_{\tau'}(\tau';p_{\tau'},q_{\tau'},\tau') = q_{\tau'}$$

$$\frac{d\bar{q}}{dt} = \bar{p}(t)/m, \; p_{\tau'}(\tau';p_{\tau'},q_{\tau'},\tau') = p_{\tau'}$$

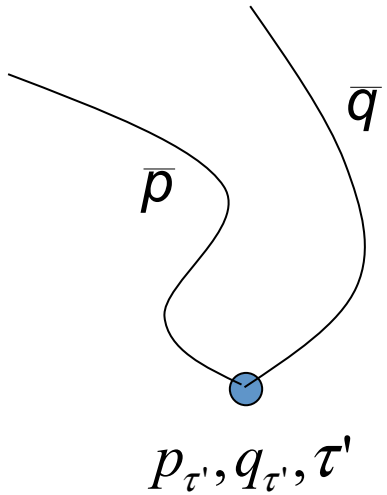

Propagator:

$$\Pi^W(p,q,t;p_{\tau'},q_{\tau'},\tau') = \delta(p - \bar{p}_t(t;p_{\tau'},q_{\tau'},\tau'))\delta(q - \bar{q}_t(t;p_{\tau'},q_{\tau'},\tau')$$

Quantum dynamics in Wigner representation

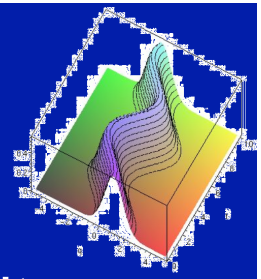

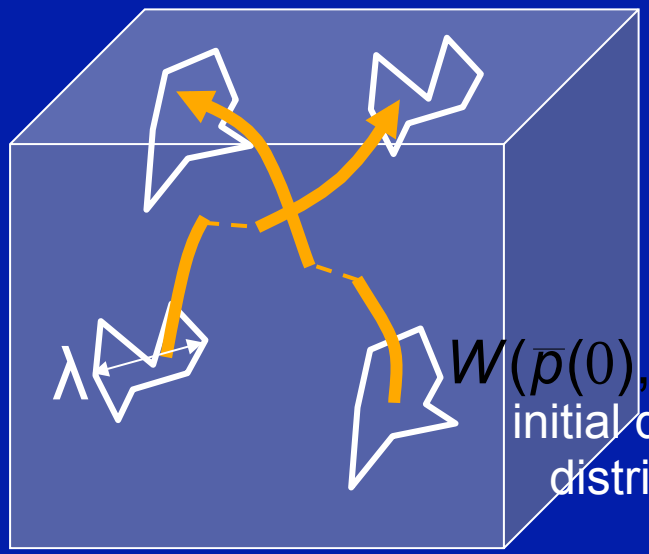

Dynamic conductivity

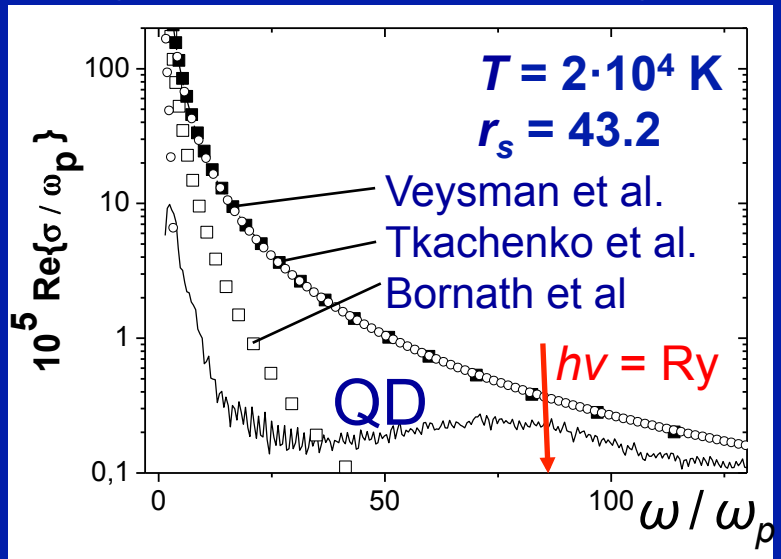

$$\frac{d\bar{p}}{dt} = \bar{F}(q(t))$$

$$\frac{d\bar{q}}{dt} = \frac{\bar{p}(t)}{m}$$

5000-20000 configurations

random momentum jumps

$$\sigma \sim FT\left(<\bar{p}(t)\bar{p}(0)>\right)$$

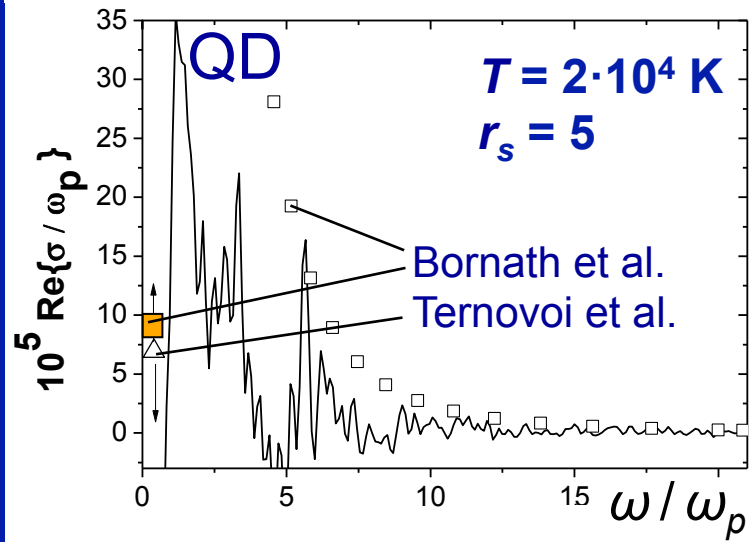

$$\sigma_{\alpha\gamma}(\omega) = \int_0^\infty dt e^{i\omega t - \epsilon t} \int_0^\beta d\lambda \left\langle \hat{J}_\gamma \hat{J}_\alpha (t + i\hbar\lambda) \right\rangle$$

Conclusions

- Ab initio methods are useful for calculation of different properties of matter at high energy density
- The main goal of ab initio methods is to replace experiment; in some cases it's already possible
- Growth of computational possibilities will allow to apply more general approaches for calculation of plasma properties (quantum filed theory)
- Currently, however, semiempirical approaches are main workhorses; ab initio methods are used for calibration of such models

Thermodynamic Functions of Thomas-Fermi Model

Free energy:

$$F(V,T)=\frac{2\sqrt{2}\upsilon_a T^{5/2}}{\pi^2}\left[I_{3/2}\left(\frac{\mu}{T}\right)-8\int_0^1 u^5 I_{3/2}(\phi)\,du+3\int_0^1 u^5\phi I_{1/2}(\phi)du\right]$$

ϕ - dimensionless atomic potential, $\phi = \phi / (u^2 T)$, υ_a – cell volume, $u = (r / r_0)^{1/2}$

Expressions for 1st derivatives of F (P and S) are known.

Second derivatives of free energy

$$P_V' = -F_{VV}'' = \frac{(2\theta)^{3/2}}{2\pi^2} I_{1/2}\left(\frac{\mu}{T}\right)\left(\mu_V'\right)_{N,T}$$

$$P_T' = -F_{VT}'' = \frac{(2\theta)^{3/2}}{2\pi^2}\left[I_{1/2}\left(\frac{\mu}{T}\right)\left(\mu_T'\right)_{N,V}+\frac{5}{3}I_{3/2}\left(\frac{\mu}{T}\right)-\frac{\mu}{T}I_{1/2}\left(\frac{\mu}{T}\right)\right]$$

$$S_T' = -F_{TT}'' = \frac{3\sqrt{2}\upsilon_a}{\pi^2 T^{3/2}}\int_0^1\left[5T^2u^5 I_{3/2}(\phi)+3u^3\left(\varphi_T' T^2-2\varphi T\right)I_{1/2}(\phi)-u\varphi\left(\varphi_T' T-\varphi\right)I_{-1/2}(\phi)\right]du$$

Shemyakin O.P. et al., JPA **43,** 335003 (2010)

Second Derivatives of the Thomas-Fermi Model

The number of particles and potential are the functions of the grand canonical ensemble variables, which are in turn depend on the variables of the canonical ensemble:

$$N = N[\mu(N,V,T),\upsilon(N,V,T),T(N,V,T)]$$

$$\varphi = \varphi[\mu(N,V,T),\upsilon(N,V,T),T(N,V,T)]$$

From the expressions for $(N'_T)_{N,\square}$, $(\square'_T)_{N,\square}$ и $(N'_{\square})_{T,N}$ one can obtain:

$$\left(\frac{\partial\mu}{\partial T}\right)_{V,N} = -\frac{(\partial N/\partial T)_{\upsilon,\mu}}{(\partial N/\partial\mu)_{\upsilon,T}}$$

$$\left(\frac{\partial\mu}{\partial V}\right)_{N,T} = -\frac{(\partial N/\partial \upsilon)_{\mu,T}}{(\partial N/\partial\mu)_{\upsilon,T}}$$

$$\left(\frac{\partial\varphi}{\partial T}\right)_{N,\upsilon} = \left(\frac{\partial\varphi}{\partial T}\right)_{\mu,\upsilon} - \frac{(\partial N/\partial T)_{\mu,\upsilon}}{(\partial N/\partial\mu)_{\upsilon,T}}\left(\frac{\partial\varphi}{\partial\mu}\right)_{\upsilon,T}$$

We need
6 derivatives in the grand canonical ensemble

$$\left(\varphi'_{\upsilon}\right)_{\mu,T} \qquad \left(\varphi'_{T}\right)_{\mu,\upsilon} \qquad \left(\varphi'_{\mu}\right)_{T,\upsilon}$$

$$\left(N'_{T}\right)_{\upsilon,\mu} \qquad \left(N'_{\mu}\right)_{T,\upsilon} \qquad \left(N'_{\upsilon}\right)_{T,\mu}$$

Shemyakin O.P. et al., JPA **43,** 335003 (2010)

TF Potential and its Derivatives on υ, μ and T

Poisson equation

$$\begin{cases} W = \varphi - u^2\mu; \\ W_u^{'} = 2uV; \\ V_u^{'} = 2au^3T^{3/2}I_{1/2}\left(\dfrac{W+u^2\mu}{Tu^2}\right); \\ W\big|_{u=0} = Z/r_0\,, W\big|_{u=1} = W_u^{'}\big|_{u=1} = 0. \end{cases}$$

$\Downarrow$

φ

Derivative of the Poisson equation on υ:

$$\begin{cases} L = \left(\varphi_\upsilon^{'}\right)_{\mu,T}; \\ L_u^{'} = 2uM; \\ M_u^{'} = \dfrac{4au^3T^{3/2}}{3\upsilon}I_{1/2}(\phi) + auT^{1/2}I_{-1/2}(\phi)L; \\ L\big|_{u=1} = L_u^{'}\big|_{u=1} = 0. \end{cases}$$

$\Downarrow$

$\left(N_\upsilon^{'}\right)_{\mu,T}$

Derivative on μ:

$$\begin{cases} \Phi = \left(\varphi_\mu^{'}\right)_{\upsilon,T} - u^2; \\ \Phi_u^{'} = auT^{1/2}\left(\Phi + u^2\right)I_{-1/2}(\phi); \\ \Psi_u^{'} = auT^{1/2}\left(\Phi + u^2\right)I_{-1/2}(\phi); \\ \Phi\big|_{u=1} = F_u^{'}\big|_{u=1} = 0. \end{cases}$$

$\Downarrow$

$\left(N_\mu^{'}\right)_{\upsilon,T}$

Derivative on T:

$$\begin{cases} Q = \left(\varphi_T^{'}\right)_{\mu,\upsilon}; \\ Q_u^{'} = 2uR; \\ R_u^{'} = au^3T^{1/2}\left[3I_{1/2}(\phi) - \phi I_{-1/2}(\phi)\right] + auT^{1/2}QI_{-1/2}(\phi); \\ Q\big|_{u=1} = Q_u^{'}\big|_{u=1} = 0. \end{cases}$$

$\Downarrow$

$\left(N_T^{'}\right)_{\mu,\upsilon}$

Adiabatic Sound Velocity by Thomas-Fermi Model

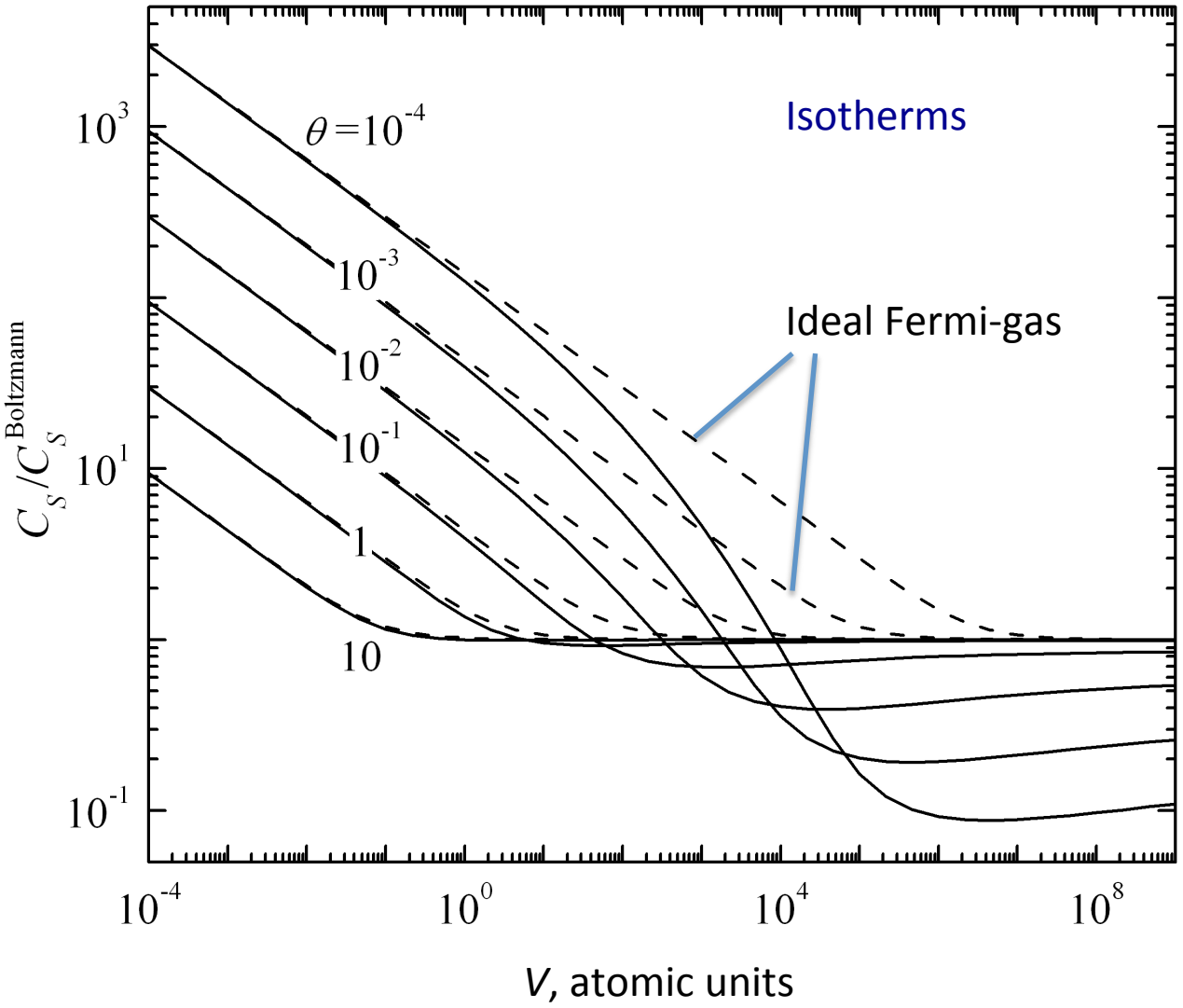

PROBLEMS OF TF MODEL

- Thomas-Fermi method is quasiclassical; if one calculates energy levels in $V_{TF}(r)$ using the Shrödinger equation and then electron density $\rho_{quant}(r)$, it will differ from the original TF electron density $\rho(r)$
- Mean ion charge is roughly determined
- The solution is to make $\rho(r)$ self-consistent and use the corrected potential and electron density

MEAN ION CHARGE (HFS)

ρ = const

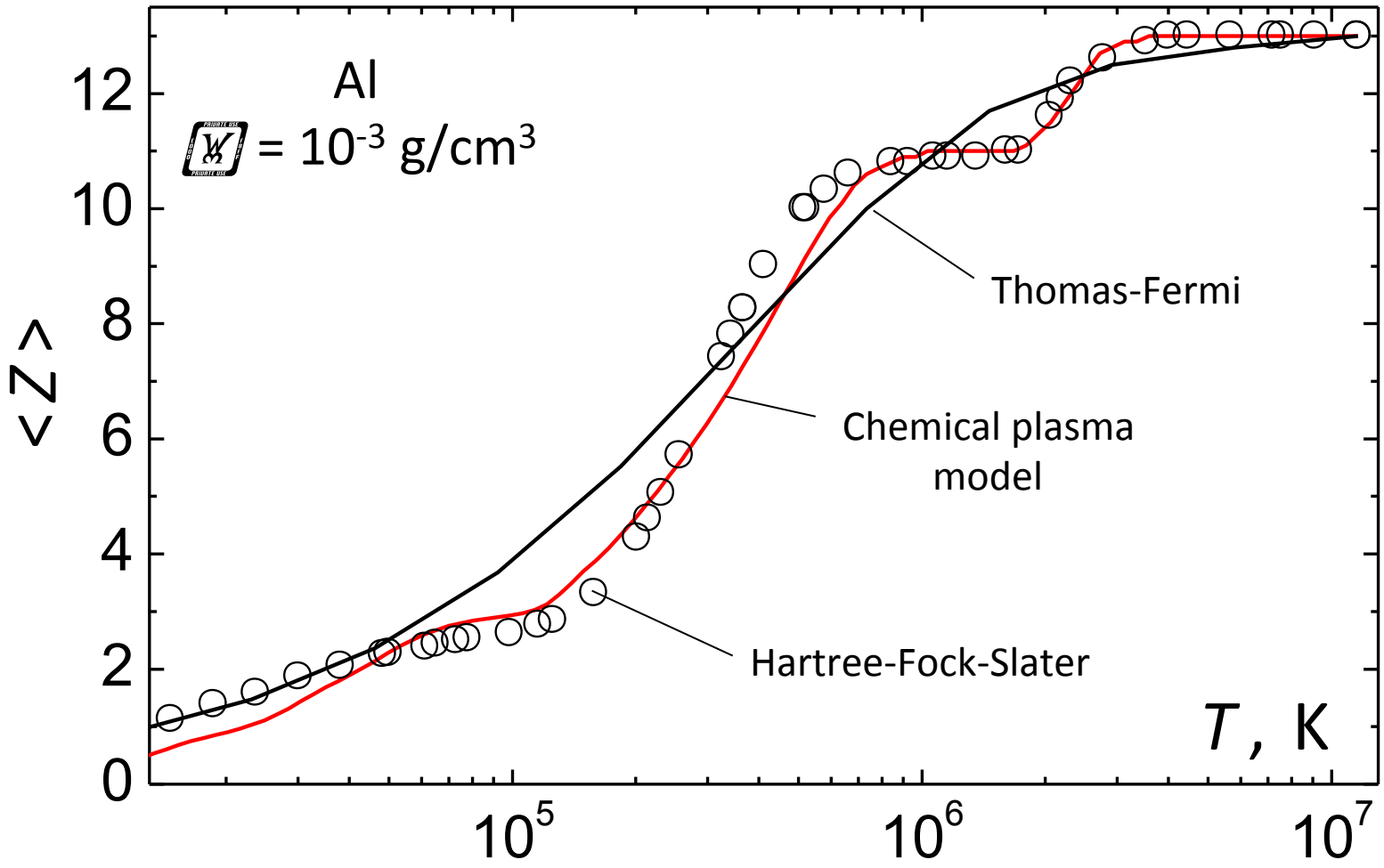

TYPICAL CONFIGURATION OF PARTICLES

H + He mixture, $T = 10^5$ K, $n_e = 10^{23}$ cm^{-3}

$$m_{\mathrm{He}} / \left(m_{\mathrm{He}} + m_{\mathrm{H}} \right) = 0.988$$

40 α-particles, 2 protons, 82 electrons

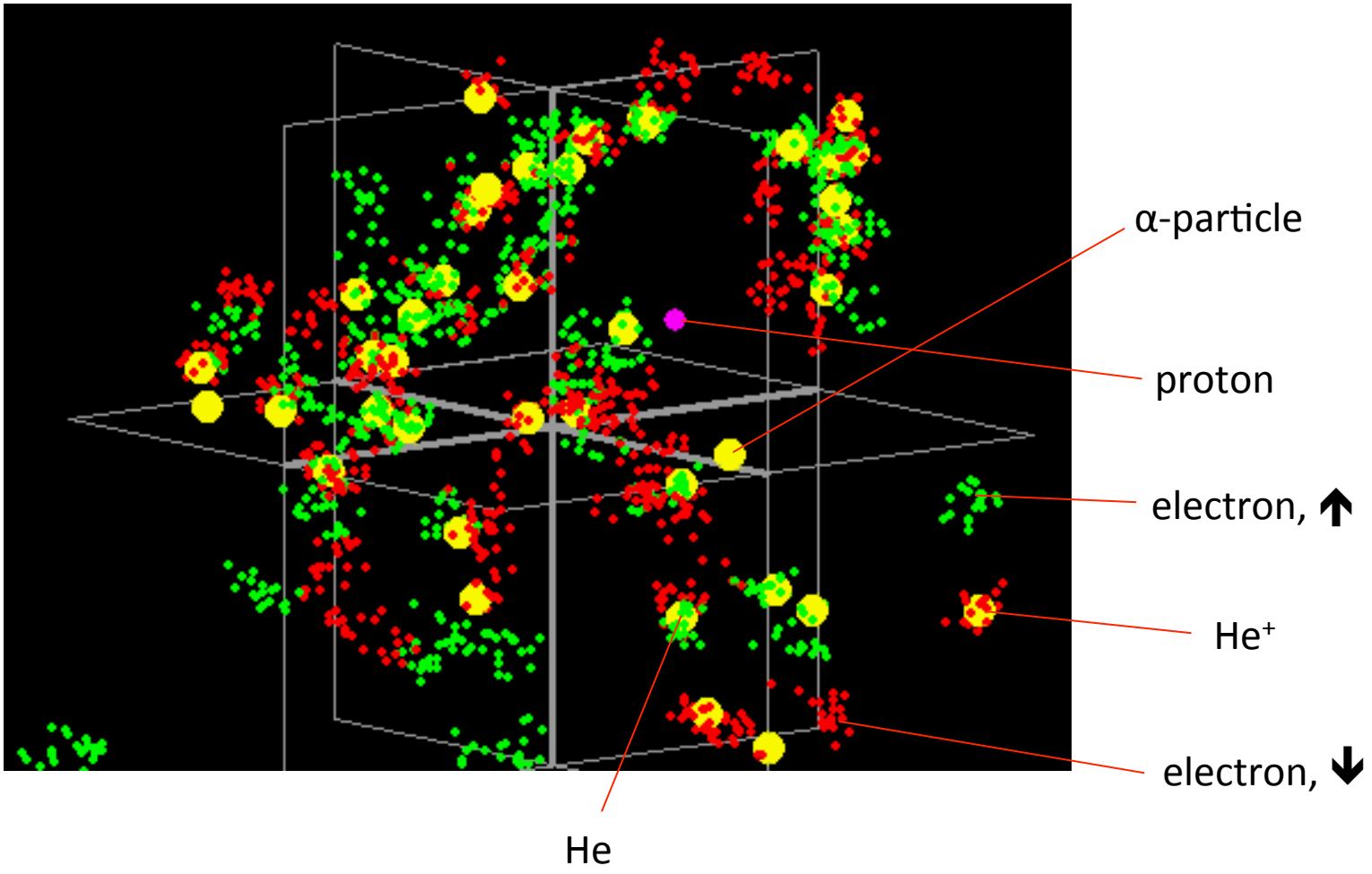

ENERGY IN H + He MIXTURE ON ISOTHERMS

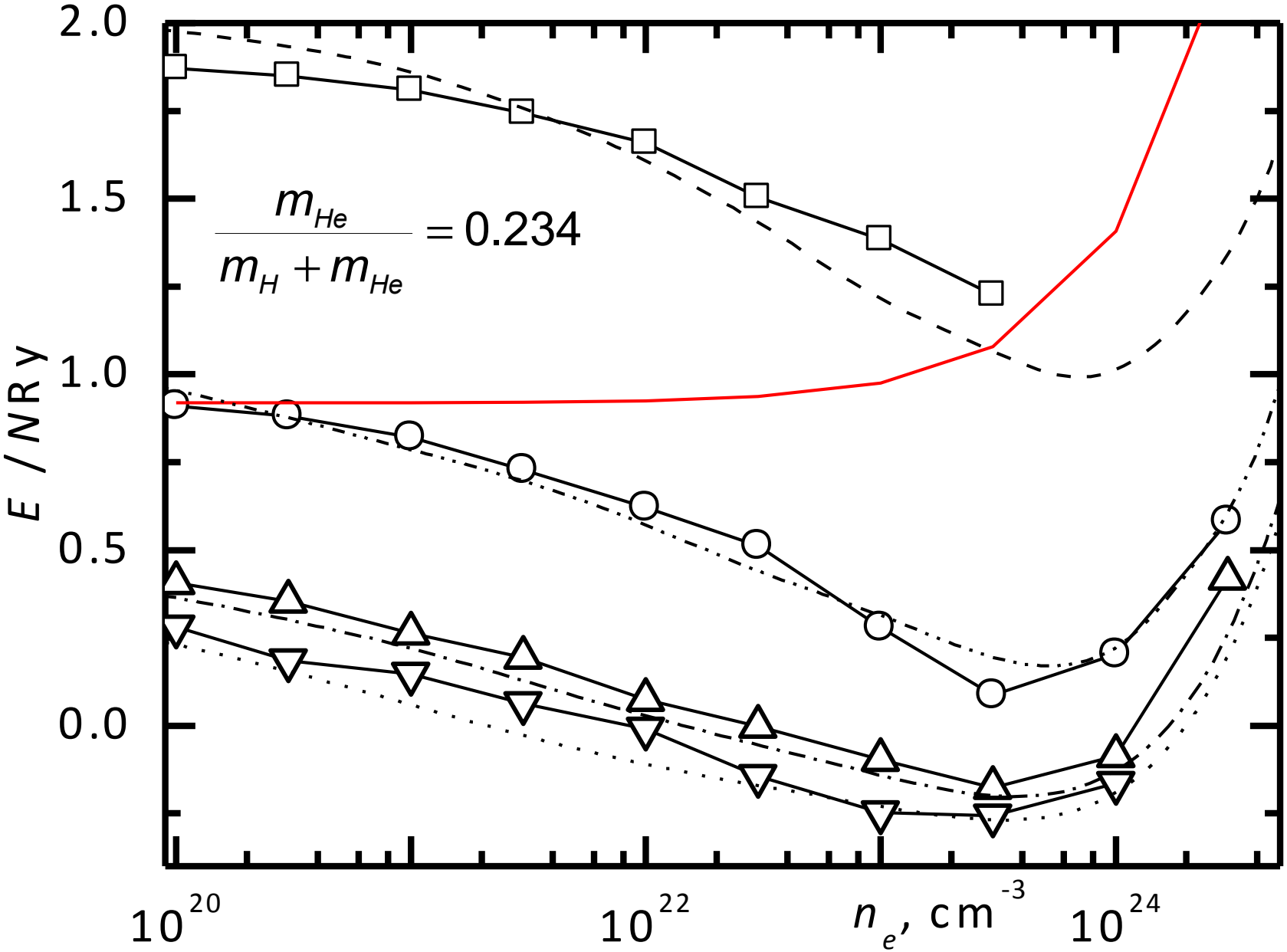

D. Saumon, G. Chabrier, H.M. Van Horn, Astrophys. J. Suppl.Ser. 1995. V.99. P.713

ELECTRON-HOLE PLASMA. PIMC SNAPSHOT

crystal, m_h(eff) = 800, m_e(eff) = 1

$\langle r \rangle / a_B = 0.63$

$T = 0.064 E_b$

- hole

- hole

- electron

- electron

ELECTRON-HOLE PLASMA. PIMC SNAPSHOT

still crystal, m_h(eff) = 100, m_e(eff) = 1

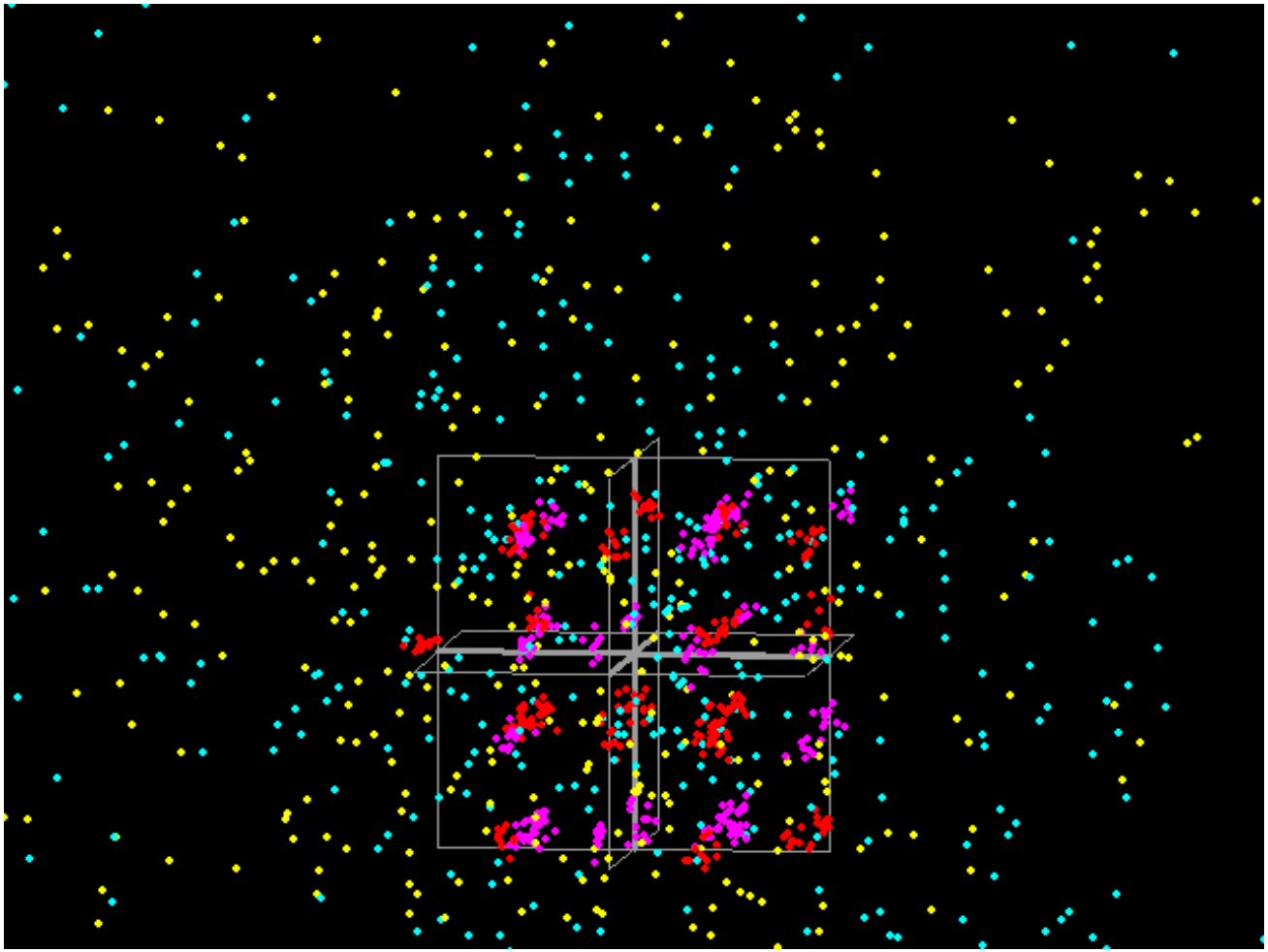

$\langle r \rangle / a_B = 0.63$

$T = 0.064 E_b$

- hole
- hole
- electron
- electron

ELECTRON-HOLE PLASMA. PIMC SNAPSHOT

liquid, m_h(eff) = 25, m_e(eff) = 1

$\langle r \rangle / a_B = 0.63$

$T = 0.064 E_b$

- hole

- hole

- electron

- electron

ELECTRON-HOLE PLASMA. PIMC SNAPSHOT

unordered plasma, m_h(eff) = 1, m_e(eff) = 1

$\langle r \rangle / a_B = 0.63$

$T = 0.064 E_b$

- hole

- hole

- electron

- electron

PAIR DISTRIBUTION FUNCTIONS. QUANTUM MELTING

$\langle r \rangle / a_B = 0.63$

$T = 0.064 E_b$

$M = m_h / m_e$

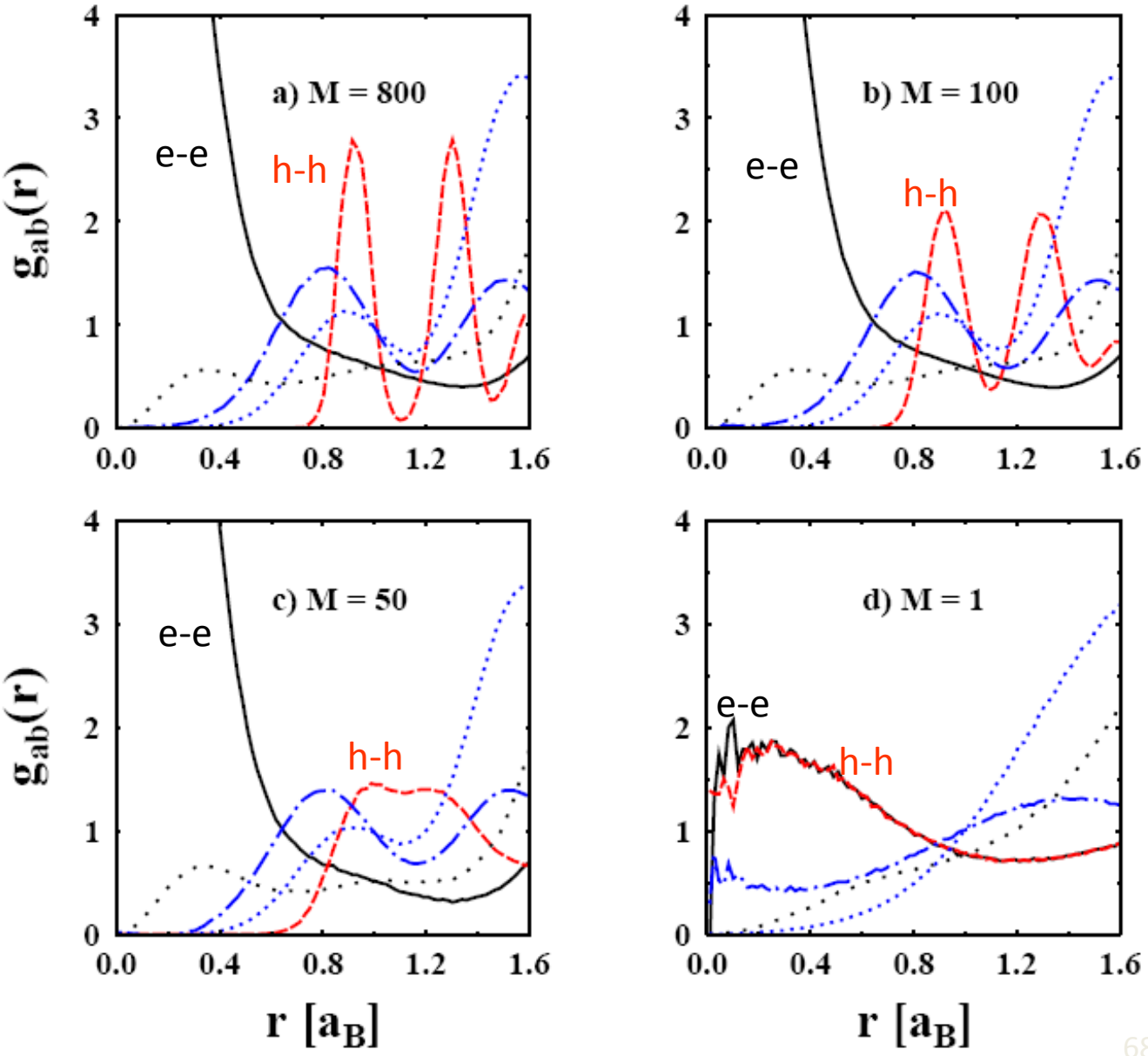

PSEUDOPOTENTIALS IN DFT

- Diminish the number of plane waves necessary for the good representation of inner electrons wave functions
- Part of electrons are considered as a core, part as valent
- Pseudopotential is constructed at $T = 0$ and doesn't depend on pressure and temperature

Pseudopotential approach

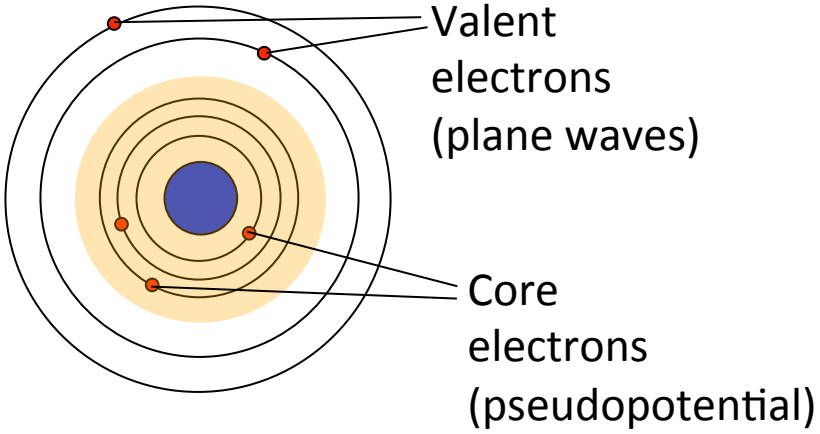

Full-potential approach

muffin-tin orbitals
for all electrons

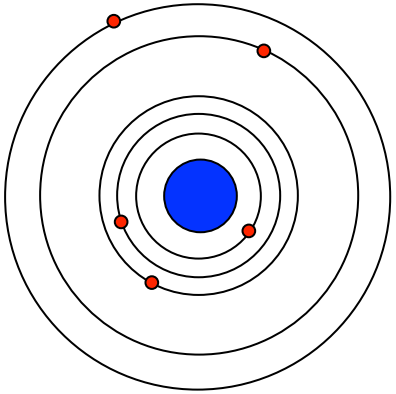

APPROXIMATIONS IN PSEUDOPOTENTIAL APPROACH

Pseudopotential describes electrons with energies less than the Fermi energy – errors at relatively high temperatures

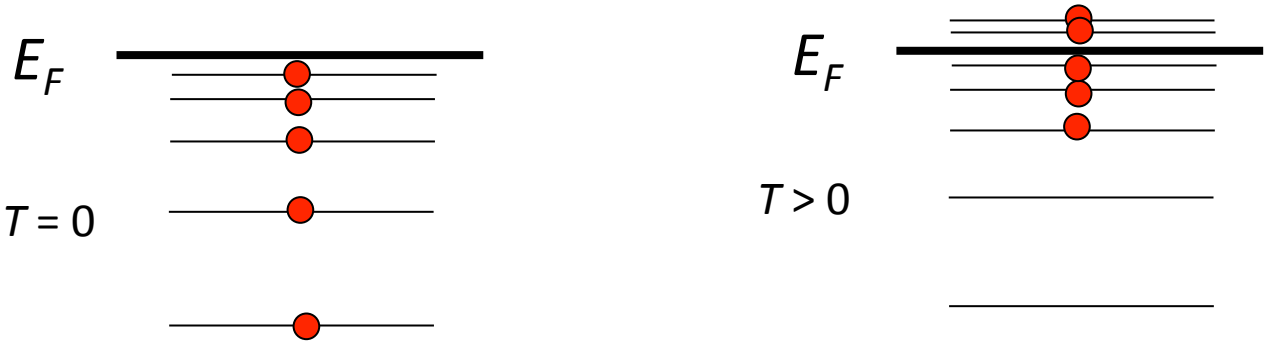

Spatial distribution of core electrons in a pseudopotential is unchanged – errors at relatively high pressures

HOLE-HOLE DISTANCE FLUCTUATIONS

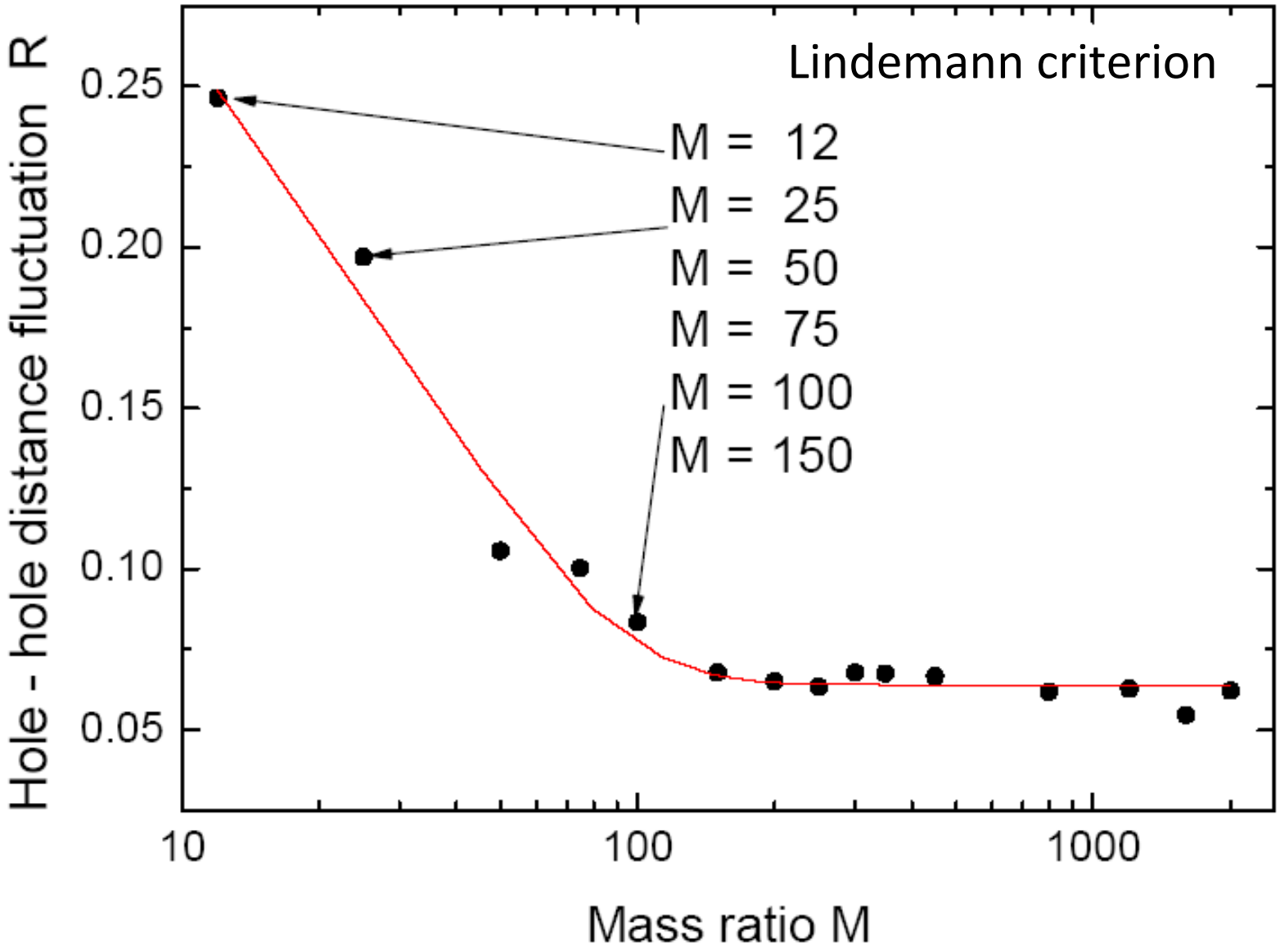

Electron Heat Capacity for W at T = 11eV. Return of Free Electrons into 4*f*-state under Compression

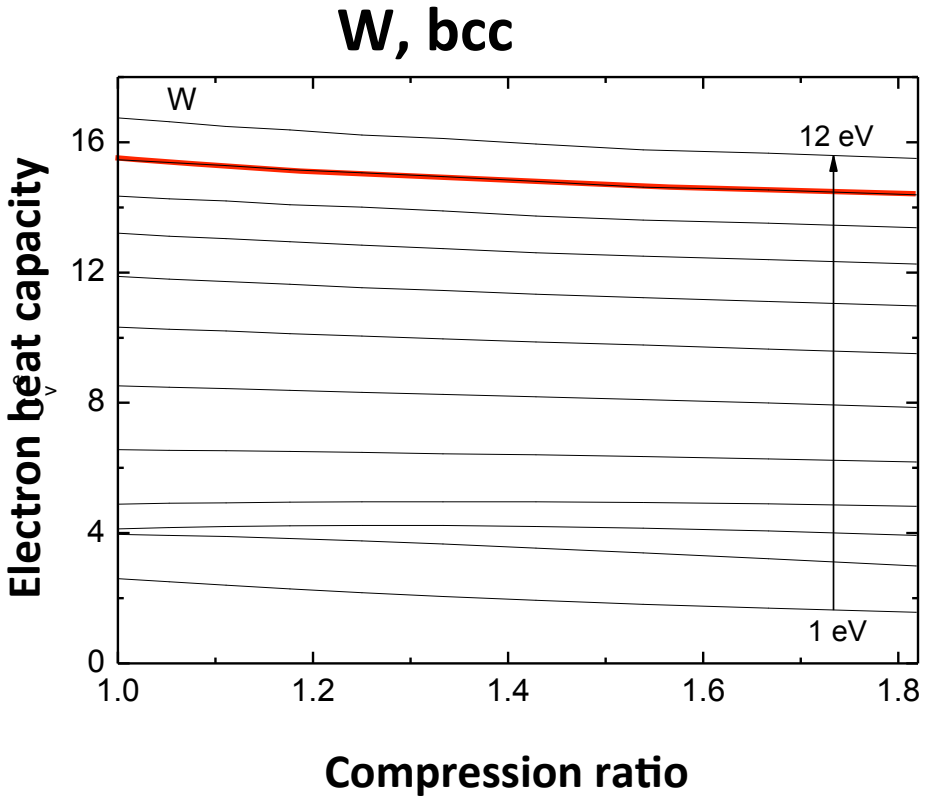

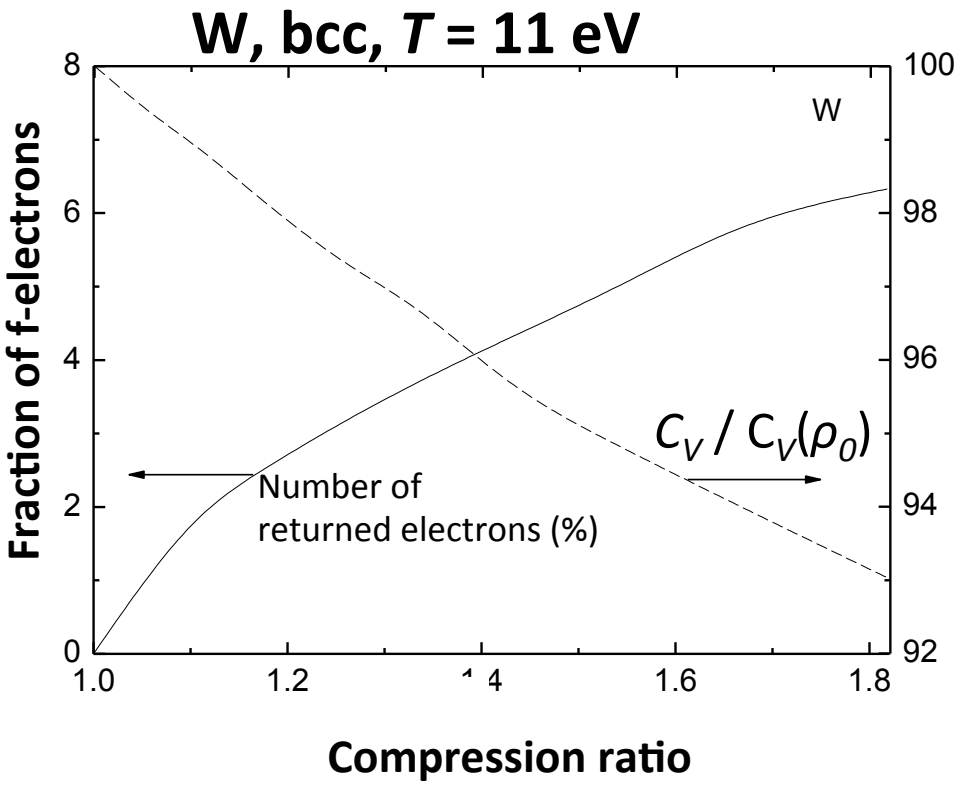

Electrons return to 4f state under compression